Cell Host & Microbe
Article

The Ubiquitin Ligase Riplet Is Essential for RIG-I-Dependent Innate Immune Responses to RNA Virus Infection

Hiroyuki Oshiumi,[1,*] Moeko Miyashita,[1] Naokazu Inoue,[2] Masaru Okabe,[2] Misako Matsumoto,[1] and Tsukasa Seya[1]
[1]Department of Microbiology and Immunology, Graduate School of Medicine, Hokkaido University, Kita-15, Nishi-7, Kita-ku Sapporo 060-8638, Japan
[2]Research Institute for Microbial Diseases, Osaka University, 3-1 Yamadaoka, Suita, Osaka 565-0871, Japan
*Correspondence: oshiumi@med.hokudai.ac.jp
DOI 10.1016/j.chom.2010.11.008

SUMMARY

RNA virus infection is recognized by the RIG-I-like receptors RIG-I and MDA5, which induce antiviral responses including the production of type I interferons (IFNs) and proinflammatory cytokines. RIG-I is regulated by Lys63-linked polyubiquitination, and three E3 ubiquitin ligases, RNF125, TRIM25, and Riplet, are reported to target RIG-I for ubiquitination. To examine the importance of Riplet in vivo, we generated Riplet-deficient mice. Fibroblasts, macrophages, and conventional dendritic cells from Riplet-deficient animals were defective for the production of IFN and other cytokines in response to infection with several RNA viruses. However, Riplet was dispensable for the production of IFN in response to B-DNA and DNA virus infection. Riplet deficiency abolished RIG-I activation during RNA virus infection, and the mutant mice were more susceptible to vesicular stomatitis virus infection than wild-type mice. These data indicate that Riplet is essential for regulating RIG-I-mediated innate immune response against RNA virus infection in vivo.

INTRODUCTION

RNA virus infection is initially recognized by RIG-I-like receptors, RIG-I and MDA5, which induce antiviral responses such as the production of type I interferons (IFNs) and proinflammatory cytokines (Yoneyama and Fujita, 2009; Takeuchi and Akira, 2010). Analyses of RIG-I and MDA5 knockout mice showed that RIG-I is essential for type I IFN production by mouse embryonic fibroblasts (MEFs), conventional dendritic cells (cDCs), and macrophages (Mfs) in response to RNA viruses such as vesicular stomatitis virus (VSV), influenza A virus (Flu), hepatitis C virus (HCV), Sendai virus (SeV), and Japanese encephalitis virus (JEV). MDA5 is critical in picornavirus infection (Kato et al., 2006; Saito et al., 2007). However, in plasmacytoid DCs (pDCs), loss of RIG-I has no effect on viral induction of IFNs, and TLR7 and MyD88 are required for inducing immune responses in these cells (Diebold et al., 2004; Kato et al., 2005; Kumar et al., 2006; Sun et al., 2006).

RIG-I consists of two N-terminal CARDs, a central DExD/H helicase domain, and a C-terminal repressor domain (CTD) (Yoneyama et al., 2004). Before viral infection, CTD of RIG-I suppresses N-terminal CARDs (Saito et al., 2007). When the CTD of RIG-I recognizes the 5′ triphosphate-double-stranded (ds) viral RNA, the conformation of the RIG-I protein changes, and the N-terminal CARD triggers interaction with its downstream partner IPS-1 (Hornung et al., 2006; Pichlmair et al., 2006; Saito et al., 2007; Cui et al., 2008; Takahasi et al., 2008; Rehwinkel et al., 2010). IPS-1 contains an N-terminal CARD that interacts with the tandem CARDs of RIG-I and a C-terminal transmembrane domain that localizes it to the mitochondrial outer membrane (Kawai et al., 2005; Meylan et al., 2005; Seth et al., 2005; Xu et al., 2005). IPS-1 activates TBK1 kinase, which mediates phosphorylation of IRF-3, leading to its dimerization and translocation into the nucleus (Kumar et al., 2006; Sun et al., 2006). The IRF-3 dimers, NF-κB, and AP-1 transcription factors activate type I IFN transcription (Honda et al., 2005). The secreted type I IFNs activates the IFNAR, which leads to phosphorylation and nuclear translocation of STAT1 (Akira et al., 2006; Honda et al., 2006).

RIG-I is regulated by ubiquitination. Three E3 ubiquitin ligases, RNF125, TRIM25, and Riplet, target RIG-I (Arimoto et al., 2007; Gack et al., 2007; Oshiumi et al., 2009). RNF125 functions as a negative regulator for RIG-I signaling and mediates Lys48-linked polyubiquitination of RIG-I, leading to protein degradation by the proteasome (Arimoto et al., 2007). On the other hand, TRIM25 and Riplet function as positive regulators for the signaling. TRIM25 mediates Lys63-linked polyubiquitination at Lys172 of RIG-I CARDs (Gack et al., 2007). Lys63-linked polyubiquitination induces interaction between RIG-I and IPS-1 CARDs, leading to the activation of signaling (Gack et al., 2007, 2008). However, there are several reports that describe other models. First, Zeng et al. developed an in vitro reconstitution system of the RIG-I pathway (Zeng et al., 2010). Using this system, they showed that Lys172 of RIG-I CARDs is required for binding to the Lys63-linked polyubiquitin chain (Zeng et al., 2010). They postulated that polyubiquitin binding and not ubiquitin modification is required for RIG-I activation (Zeng et al., 2010). In their model, unanchored polyubiquitin chains are responsible for RIG-I activation. However, they did not rule out the possibility that ubiquitination of some signaling proteins may contribute to RIG-I activation (Zeng et al., 2010). Second, Fujita T and his colleagues reported that residue 172 of mouse RIG-I is not Lys but Gln and human RIG-I K172R mutant was normally activated by SeV infection in RIG-I KO MEFs (Shigemoto et al., 2009).

The third ubiquitin ligase, Riplet, mediates Lys63-linked polyubiquitination of RIG-I CTD and CARDs (Gao et al., 2009; Oshiumi et al., 2009). This polyubiquitination promotes RIG-I activation and its antiviral activity in human cells (Horner and Gale, 2009; Nakhaei et al., 2009; Takeuchi and Akira, 2010; Yoneyama and Fujita, 2010); however, in vivo evidence is absent. Type I IFNs are mainly produced by DCs or Mf in vivo, and RIG-I is essential for type I IFN production in cDC and Mf (Kato et al., 2005; Sun et al., 2006; Kumagai et al., 2007). The role of Riplet in these cells also has not yet been examined. Both TRIM25 and Riplet proteins mediate Lys63-linked polyubiquitination of RIG-I, and thus Gao et al. suggested that Riplet may be a complementary factor of TRIM25 for RIG-I activation (Gao et al., 2009). Therefore, it is not known whether Riplet is essential for RIG-I activation. To address these issues, we generated Riplet knockout mice. Our analysis revealed that Riplet is essential for the RIG-I activation and innate immune responses against viral infection in vivo.

RESULTS

Ubiquitous Expression of Riplet mRNA

First, we examined mouse Riplet mRNA expression by quantitative PCR (qPCR), and found it to be ubiquitously expressed in various tissues, MEFs, bone marrow-derived DCs (BM-DCs), and Mf (BM-Mf) (Figure 1A, left panel). Furthermore, we have previously shown that human Riplet mRNA is expressed in various tissues. When we examined the expression of Riplet mRNA in human DCs, it was observed in human DCs as in HeLa cells (Figure 1A, right panel). These data indicate that Riplet is expressed in various tissues and cells that are able to produce type I IFNs.

Generation of Riplet-Deficient Mice

Previously, we have shown that Riplet is a positive regulator for RIG-I-mediated signaling, and it mediates Lys63-linked polyubiquitination of RIG-I. However, the functional role of Riplet in vivo remains unclear. To investigate the role of Riplet in vivo, we generated Riplet-deficient (*Riplet*$^{-/-}$) mice by homologous recombination of embryonic stem cells (ESCs) (Figure 1B). We confirmed the target disruption of Riplet without deletion outside the targeted region (Figure 1C, and see Figures S1A and S1B available online). Riplet mRNA expression was abolished in *Riplet*$^{-/-}$ cells (Figures 1E and 1F), and the knockout of Riplet did not affect the expression of other genes, such as RIG-I, MDA5, IPS-1, TICAM-1, TLR3, and TRIM25, which are involved in type I IFN production (Figure 1F). The mutant mice were born at the Mendelian ratio from *Riplet*$^{+/-}$ parents (Figure 1D), and they developed and bred normally. These mice displayed no apparent abnormalities up to 7 months of age. Mutations in the human Riplet/RNF135 gene cause the overgrowth syndrome (Douglas et al., 2007). We did not observe any overgrowth phenotypes in *Riplet*$^{+/-}$ and *Riplet*$^{-/-}$ mice. Next, we examined the composition of CD4-, CD8-, CD11c-, and/or PDCA1-positive cells in the spleen, and found no difference between wild-type and *Riplet*$^{-/-}$ mice (Figures S1C and S1D). Induction of cDC from BM in the presence of GM-CSF was also normal in *Riplet*$^{-/-}$ mice (Figure S1E). Therefore, the mouse Riplet gene is dispensable for development.

Riplet$^{-/-}$ Embryonic Fibroblasts Are Defective in Innate Immune Responses against RNA Viruses

Riplet is a positive regulator for RIG-I-mediated signaling. In mouse fibroblast, VSV and Flu are mainly recognized by RIG-I (Kato et al., 2006). Furthermore HCV 3′UTR RNA is also recognized by RIG-I (Saito et al., 2008). Therefore, we first examined the expression of type I IFNs, IFN-inducible gene IP-10, and Ccl5 in MEFs after HCV 3′UTR dsRNA transfection or infection with VSV or Flu. The induction of mRNA of IFN-α2, -β, IP-10, and Ccl5 in response to VSV or Flu was abrogated in *Riplet*$^{-/-}$ MEFs (Figures 2A–2D). In addition, transfection of low concentration of HCV 3′UTR dsRNA (0.05–0.2 μg/well) also failed to upregulate IFN-α2, -β, and IFN-inducible genes in *Riplet*$^{-/-}$ MEFs (Figures 2A–2D).

Single-stranded (ss) RNA, which is synthesized by T7 RNA polymerase in vitro, induced lower IFN-β expression than dsRNA (Figure S2A). The induction of IFN-β mRNA by HCV 3′UTR ssRNA was also abolished in *Riplet*$^{-/-}$ MEFs (Figure S2A). Although the induction of IFN-β mRNA in response to VSV infection was abrogated in *Riplet*$^{-/-}$ MEFs even at high (moi = 5) or low multiplicities of infection (moi = 0.2 or 1), the induction of IFN-β mRNA in response to high concentration of HCV dsRNA (0.8 μg/well) was detected in *Riplet*$^{-/-}$ MEFs (Figures S2C–S2K). Therefore, RIG-I does not require Riplet function in the presence of large amounts of naked viral RNA in the cytoplasmic region.

Recently, Onoguchi et al. reported that type III IFN, IFN-λ, induction was RIG-I dependent during viral infection (Onoguchi et al., 2007). The induction of IFN-λ mRNA in response to VSV was also abrogated in *Riplet*$^{-/-}$ MEFs (Figure S2B).

Next, we examined type I IFNs or IL-6 levels in culture supernatants after viral infection or HCV 3′UTR RNA transfection (low concentration condition). The production of IFN-α, -β, and IL-6 in culture supernatants was abrogated in *Riplet*$^{-/-}$ MEFs (Figures 3A–3C). Next, we analyzed the contribution of Riplet to the antiviral response. When MEFs were infected with VSV at various mois, cytopathic effects (CPEs) were more severe in *Riplet*$^{-/-}$ than in wild-type MEFs (Figure 3D). These results demonstrate that Riplet plays a critical role in the elimination of RNA virus infection by induction of IFN responses.

Riplet Is Dispensable for the Production of Type I IFN Induced by B-DNA and HSV-1 Infection

Cytoplasmic B-form double-stranded DNA (dsDNA) stimulates the cells to induce type I IFNs and IFN-inducible genes (Ishii et al., 2006). TBK1 is required for type I IFN induction by dsDNA (Ishii et al., 2008). Although immortalized MEFs require RIG-I for type I IFNs production by dsDNA stimulation, primary MEFs do not require IPS-1, which is a RIG-I adaptor, for type I IFNs production by dsDNA (Kumar et al., 2006; Chiu et al., 2009). We examined the expression of IFN-β and IP-10 mRNA by dsDNA stimulation in primary wild-type and *Riplet*$^{-/-}$ MEFs. IFN-β and IP-10 mRNA were detected in *Riplet*$^{-/-}$ MEFs by dsDNA transfection similar to that detected in wild-type MEFs (Figures 4A and 4B).

Next, we examined IFN-β mRNA expression during infection with DNA virus, HSV-1. Wild-type and *Riplet*$^{-/-}$ MEFs were infected with HSV-1, and IFN-β mRNA expression was examined by RT-qPCR. IFN-β expression in *Riplet*$^{-/-}$ MEFs was comparable to that in wild-type MEFs (Figure 4C). Taken together, these

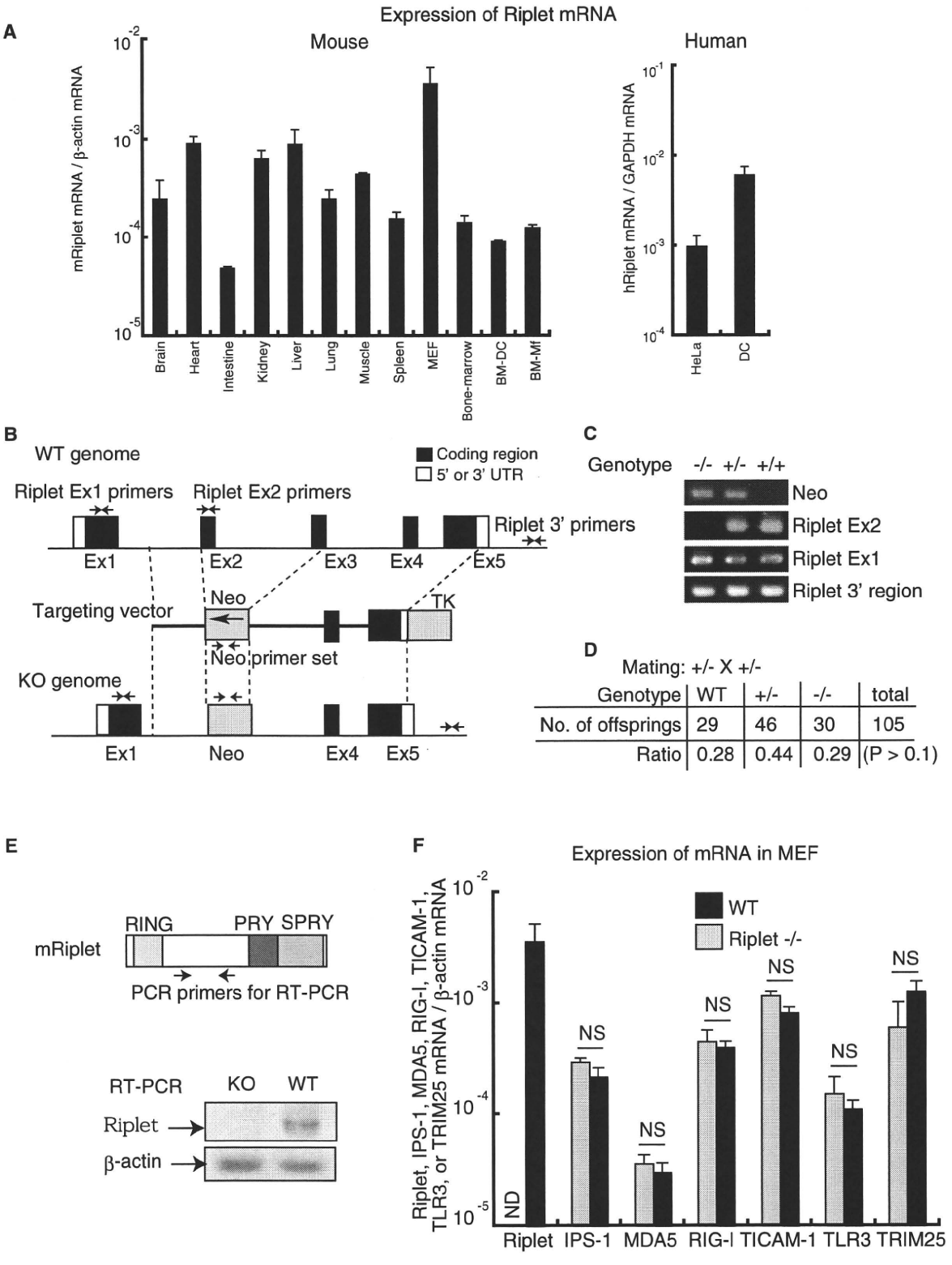

Genotype	WT	+/-	-/-	total
No. of offsprings	29	46	30	105
Ratio	0.28	0.44	0.29	(P > 0.1)

Figure 1. Targeted Disruption of the Murine Riplet Gene

(A) Riplet mRNA expression in mouse tissues and cells or human cells. RT-qPCR was performed to measure Riplet mRNA, and each sample was normalized to β-actin (mouse) or GAPDH (human). Data are shown as means ±SD and are representative of three independent experiments.

(B) Structure of the mouse Riplet gene, targeting vector, and disrupted gene. Closed boxes indicate the coding exon of Riplet, and hatched boxes indicate the Neo or TK gene coding region. The primer sets for PCR are shown by arrows.

data indicate that Riplet-dependent RIG-I activation is dispensable for type I IFN and IFN-inducible genes mRNA expression by cytoplasmic DNA in primary MEFs. This is consistent with previous studies reporting that the IPS-1-dependent pathway is dispensable for type I IFN production by cytoplasmic dsDNA stimulation (Kumar et al., 2006).

Riplet Is Essential for Triggering the RIG-I Signaling Pathway

We further examined the role of Riplet in RIG-I-mediated signaling during RNA virus infection. In RIG-I-mediated signaling, induction of type I IFNs and proinflammatory cytokines requires the activation of transcription factor IRF3. IRF3 is phosphorylated by TBK1 and IKK-ε. Phosphorylated IRF3 induces IFN-β gene expression. IFN-β produced subsequently stimulates the JAK-STAT pathway to amplify the responses. To determine the role of Riplet in signaling pathway activation, we analyzed IRF3 and STAT1 activations after VSV infection in *Riplet*$^{-/-}$ MEFs. VSV-induced dimerization of IRF3 and VSV- or Flu-induced pohsphorylation of STAT1 were abrogated in *Riplet*$^{-/-}$ MEFs (Figures 3E and 3F). These results demonstrate that Riplet is essential for activating the transcription factors that work early phase of RNA virus infection.

In the absence of viral infection, RIG-I CTD suppressed N-terminal CARDs (Saito et al., 2007). After viral infection, RIG-I CTD binds to viral RNA, leading to conformational changes (Saito et al., 2007). Later, RIG-I CARDs undergo TRIM25-mediated polyubiquitination and associate with IPS-1 CARD (Gack et al., 2007, 2008). When we tested the effect of Riplet on RIG-I activation, the full-length RIG-I protein with CTD failed to activate the IFN-β promoter in *Riplet*$^{-/-}$ MEFs (Figure 5A); however, promoter activation by the expression of RIG-I CARDs without CTD was normal in *Riplet*$^{-/-}$ MEFs (Figure 5B). These data indicate that Riplet is required for the activation of full-length RIG-I, but not for the activation of RIG-I CARDs without CTD. Next, we performed complementation assays. Immortalized *Riplet*$^{-/-}$ MEFs were transfected with an empty-, RIG-I-, or RIG-I-5KA mutant-expressing vector together with or without Riplet-expressing vector. The RIG-I-5KA mutant harbors mutations in five C-terminal Lys residues that are important for Riplet-mediated ubiquitination (Oshiumi et al., 2009). In the *Riplet*$^{-/-}$ cell line, RIG-I was not activated by HCV RNA stimulation, and Riplet expression led to the activation of wild-type RIG-I (Figure 5C). The deletion of the Riplet RING finger domain, which is the catalytic domain of ubiquitin ligase, abolished RIG-I activation (Figure 5D). Unlike wild-type RIG-I, Riplet expression failed to activate the RIG-I-5KA mutant protein (Figure 5C). The activations of wild-type and mutant RIG-I were correlated with its polyubiquitination (Figure S3A). Although the RNA binding activity was weakly reduced by the 5KA mutation, the pull-down assay showed that RIG-I-5KA mutant bound to dsRNA (Figure S3B). Next, we examined ligand-independent RIG-I activation by overexpression of Riplet. Overexpression of Riplet in HEK293 cells activated RIG-I in the absence of RIG-I ligand, such as viral RNA (Figure S3C). This ligand-independent activation of RIG-I by Riplet overexpression was also abolished by the 5KA mutation (Figure S3C). In addition, we examined the polyubiquitination of exogenously expressed RIG-I CTD fragment. Polyubiquitination of RIG-I CTD fragment was increased by overexpression of Riplet (Figure 5M), and was reduced by overexpression of the dominant-negative form of Riplet (Riplet DN) (Figure 5N). Polyubiquitination of RIG-I CTD fragment was not detected in Riplet-deficient cells (R3T cells); however, expression of Riplet led to polyubiquitination of RIG-I CTD fragment (Figure 5O). These data are consistent with our previous report (Oshiumi et al., 2009). Taken together, these data indicate that Riplet-dependent polyubiquitination of RIG-I is important for RIG-I activation.

Previously, we showed that Riplet is not involved in MDA5-mediated signaling. IFN-β promoter activation by MDA5 overexpression was normal in *Riplet*$^{-/-}$ MEFs (Figure 5E). Transfection of poly(I:C), which is recognized by MDA5, induced IFN-β, IL-6, and IP-10 expression in both wild-type and *Riplet*$^{-/-}$ MEFs (Figures 5F–5H). In addition, stimulation with lipopolysaccharide (LPS), which is a TLR4 ligand, normally induced expression of these cytokines in *Riplet*$^{-/-}$ MEFs (Figures 5I–5K). Furthermore, IL-6 production in culture medium in response to LPS was normal in *Riplet*$^{-/-}$ MEFs (Figure 5L). Taken together, these data indicate that Riplet is essential for the RIG-I-mediated type I IFN or IL-6 production upon viral infection in nonprofessional immune cells like fibroblasts, but is not required for MDA5- or TLR4-mediated signaling.

Riplet Is Required for Antiviral Innate Immune Responses in Conventional Dendritic Cells and Macrophages

We examined whether Riplet is required for the induction of type I IFN in DCs or Mf. DCs play a pivotal role in bridging innate and adaptive immune responses, and can be classified into cDCs and pDCs, the latter producing high levels of type I IFNs. Mfs also produce type I IFN. We induced cDCs from BM cells in the presence of GM-CSF (BM-DC). Twenty-four hours after VSV or Flu infection, cDCs of wild-type mice produced IFN-α, -β, and IL-6 (Figures 6A–6F). In contrast, the cDCs of *Riplet*$^{-/-}$ mice showed severely impaired IFN-α, -β, or IL-6 production during VSV or Flu infection (Figures 6A–6F). When the cDCs were stimulated with a TLR4 ligand, such as LPS, IFN-β or IL-6 production in *Riplet*$^{-/-}$ cDCs was almost normal (Figures S4A and S4B), indicating that Riplet is dispensable for LPS-induced cytokine production in cDCs.

Then we tested M-CSF-induced BM-Mf. Wild-type Mf produced IFN-α, -β, and IL-6 after VSV or Flu infection (Figures

(C) PCR of mouse tail. Genomic DNA was extracted from wild-type, *Riplet*$^{+/-}$, or *Riplet*$^{-/-}$ mice tails and PCR was performed using primers shown in (B).
(D) Genotype analyses of offspring from heterozygote intercrosses. Chi-square goodness-of-fit test indicated that deviation from Mendelian ratio was not statistically significant ($p > 0.1$).
(E) RT-PCR of MEFs. Total RNA from wild-type and *Riplet*$^{-/-}$ MEFs were extracted and subjected to RT-PCR to determine Riplet mRNA expression.
(F) Riplet, IPS-1 MDA5, RIG-I, TICAM-1, TLR3, and TRIM25 expression in MEFs. Total RNA from wild-type and *Riplet*$^{-/-}$ MEFs were extracted and subjected to RT-qPCR to determine mRNA expression. Expression of the indicated gene mRNA was normalized to β-actin mRNA expression. Data are shown as means ±SD and are representative of three independent experiments. "NS" indicates no statistically significant difference between the two samples.
See also Figure S1 and Table S1.

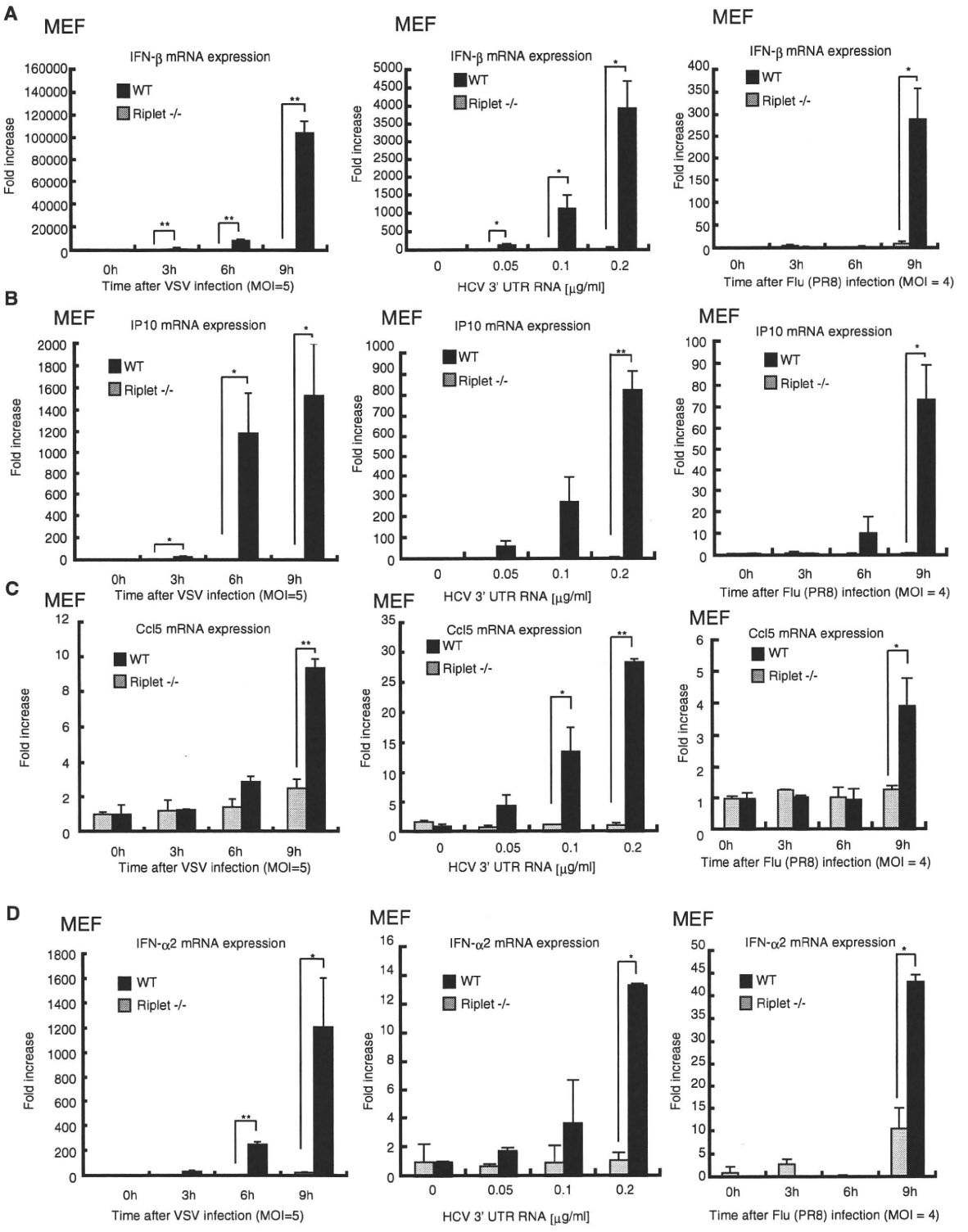

Figure 2. Abolished Responses to RNA Virus Infection in *Riplet*$^{-/-}$ Fibroblasts

Wild-type or *Riplet*$^{-/-}$ MEFs were infected with VSV or influenza A virus (Flu), and total RNA was extracted at the indicated times. Short HCV 3′UTR dsRNA was transfected into wild-type or *Riplet*$^{-/-}$ MEFs, and total RNA was extracted after 24 hr. Extracted RNA was subjected to RT-qPCR to determine IFN-β (A), IP10 (B), Ccl5 (C), or IFN-α2 (D) expression. Expression of each sample was normalized to β-actin mRNA expression. Data are shown as means ±SD and are representative of three independent experiments. *$p < 0.05$, **$p < 0.01$ (t test).

See also Figure S2 and Table S1.

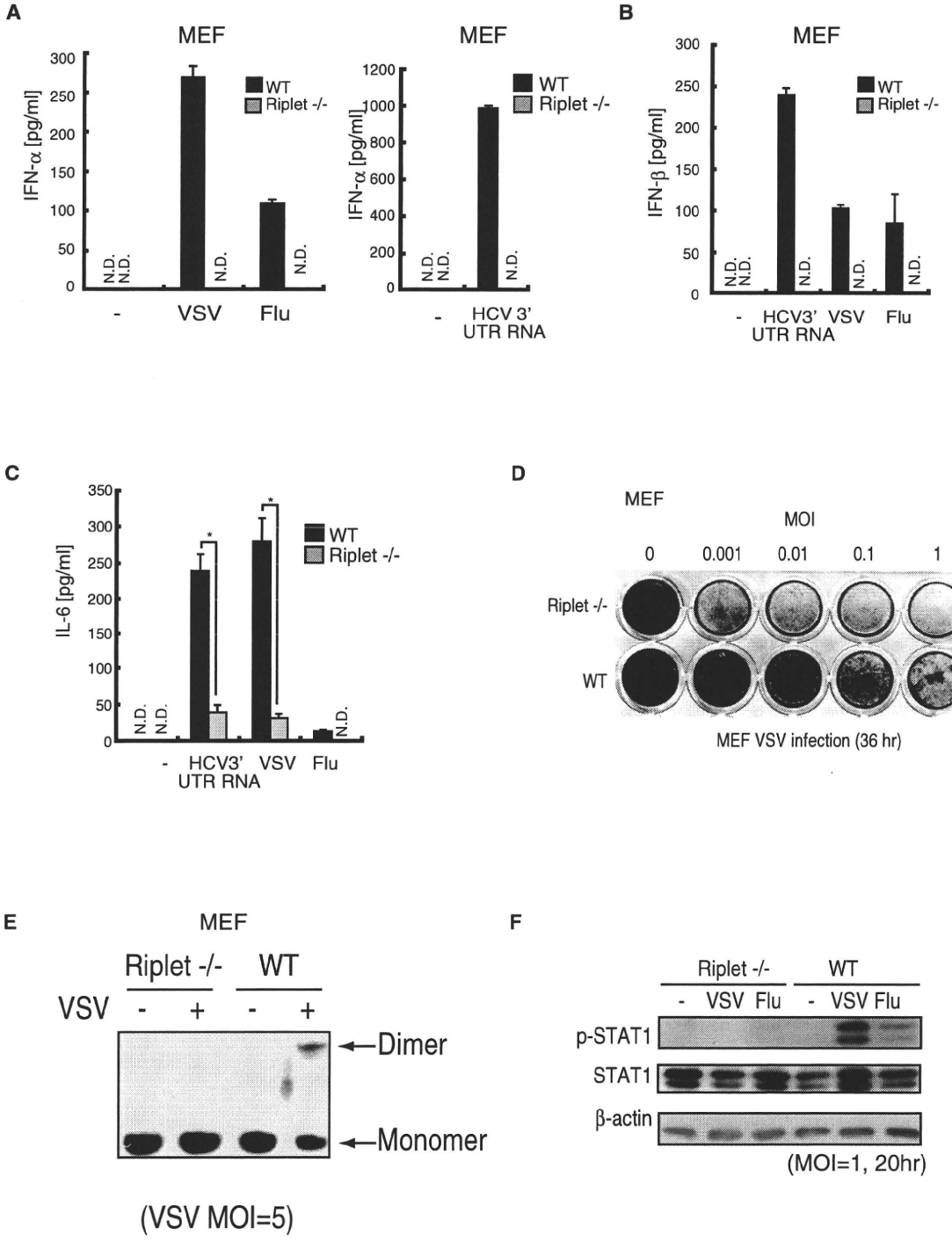

Figure 3. Role of Riplet in Antiviral Responses in Fibroblasts

(A–C) Wild-type or *Riplet*$^{-/-}$ MEFs were infected with VSV or Flu or transfected with short HCV 3′UTR dsRNA. Amounts of IFN-α (A), -β (B), and IL-6 (C) in culture supernatants were measured by ELISA after 24 hr. Data are shown as means ±SD and are representative of three independent experiments. *$p < 0.05$, **$p < 0.01$ (t test).

(D) Wild-type or *Riplet*$^{-/-}$ MEFs were infected with VSV at the indicated moi, and after 36 hr MEFs were fixed with formaldehyde and stained with crystal violet.

(E) Wild-type or *Riplet*$^{-/-}$ MEFs were infected with VSV at moi = 5, and after 9 hr cell lysates were prepared and analyzed by native PAGE. IRF-3 proteins were stained with anti-IRF3 antibody.

(F) Wild-type or *Riplet*$^{-/-}$ MEFs were infected with VSV or Flu at moi = 1, and after 20 hr cell lysates were prepared. The samples were analyzed by SDS-PAGE and western blotting. They were stained with anti-STAT1, phospho-STAT1, or β-actin antibodies.

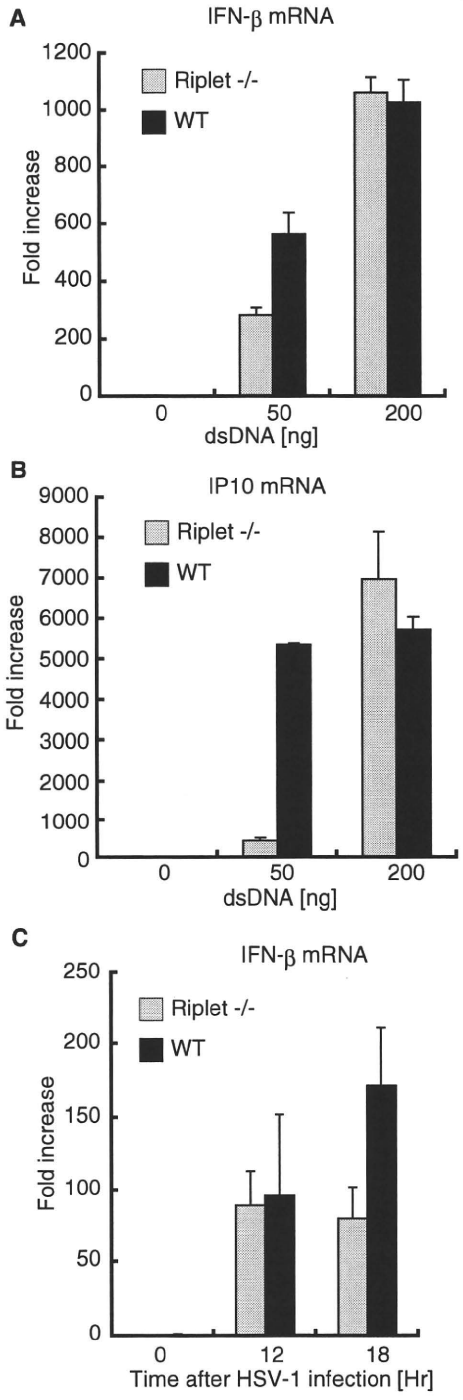

Figure 4. Role of Riplet in Type I IFN Production Induced by Cytoplasmic dsDNA

(A and B) Wild-type and *Riplet*$^{-/-}$ MEFs were transfected with the indicated amounts of dsDNA (Salomon sperm DNA) using the Lipofectamine 2000 reagent. Nine hours after the transfection, IFN-β (A) and IP-10 (B) mRNA expression was determined by RT-qPCR. Data are shown as means ±SD and are representative of three independent experiments.

(C) Wild-type and *Riplet*$^{-/-}$ MEFs were infected with HSV-1 at moi = 4, and IFN-β mRNA expression at the indicated times was examined by RT-qPCR. Data are shown as means ±SD and are representative of three independent experiments.

6A–6F). Similar to cDCs, cytokine production was reduced in Riplet knockout mice (Figures 6A–6F). Peritoneal Mf were isolated from wild-type and *Riplet*$^{-/-}$ mice. Knockout of Riplet reduced type I IFN production from peritoneal Mfs during VSV infection (Figures S4C and S4D).

We next generated Flt3L-induced DCs (Flt3L-DCs), which contain pDCs. Akira and his colleagues previously showed that the knockout of RIG-I or IPS-1 does not reduce type I IFN and IL-6 production by Flt3L-DCs, because RIG-I is dispensable for cytokine production in pDCs (Kato et al., 2005). The Flt3L-DCs of *Riplet*$^{-/-}$ mice produced normal amounts of IFN-a, -β, and IL-6 during Flu infection (Figures 6A–6F). This is consistent with the notion that Riplet is essential for the RIG-I-mediated type I IFNs and IL-6 production. Although the IFN-α levels in the culture medium after VSV infection were comparable with those in wild-type and *Riplet*$^{-/-}$ mice, Flt3L-DCs of *Riplet*$^{-/-}$ mice produced less IL-6 compared with that produced by wild-type mice through an unknown mechanism (Figure 6C).

Next, we examined type I IFN production during SeV infection. SeV infection induced IFN-α and -β productions from wild-type BM-DC, and the knockout of Riplet reduced IFN-α and -β productions from BM-DC (Figures S4E–S4J). Wild-type Flt3L-DC produced IFN-α after SeV infection, and the knockout of Riplet did not reduce IFN- α production from Flt3L-DC (Figures S4E–S4J).

Riplet Is Essential for Antiviral Immune Defense In Vivo

To investigate the role of Riplet in antiviral responses in vivo, wild-type and *Riplet*$^{-/-}$ mice were injected intraperitoneally with wild-type VSV, and sera were collected to measure type I IFN and IL-6 levels. IFN-α, -β, and IL-6 levels in sera were markedly reduced in *Riplet*$^{-/-}$ mice compared to in wild-type mice (Figures 7A and 7B, and Figure S5A). Next, wild-type and *Riplet*$^{-/-}$ mice were intranasally infected with VSV, and type I IFN levels in their sera were measured. At early time points, IFN-α and -β production was reduced in *Riplet*$^{-/-}$ mice compared to wild-type mice (Figures 7C and 7D); however, cytokine levels were comparable at later time points (Figures S5B and S5C). Previously, Ishikawa et al. observed that the knockout of STING gene, which is involved in RIG-I-dependent signaling, leads to reduction of type I IFN at early time points and relatively less reduction at later time points (Ishikawa and Barber, 2008; Ishikawa et al., 2009).

To determine if Riplet deficiency affects the survival of mice after VSV infection, the mice were intranasally infected with VSV, and their survival was monitored. Wild-type mice survived VSV infection; however, *Riplet*$^{-/-}$ mice were susceptible to VSV infection (Figure 7E). The viral titer in *Riplet*$^{-/-}$ mice brains 7 days after infection was higher than in wild-type mice (Figure 7F). These data indicate that Riplet plays a key role in the host defenses against VSV infection in vivo, and type I IFN production at early time points is important for host defenses.

DISCUSSION

In this study, we presented genetic evidence that Riplet is indispensable for antiviral responses in MEFs, BM-Mf, and BM-DCs, but not in Flt3L-DCs. The cell-type-specific requirement of Riplet

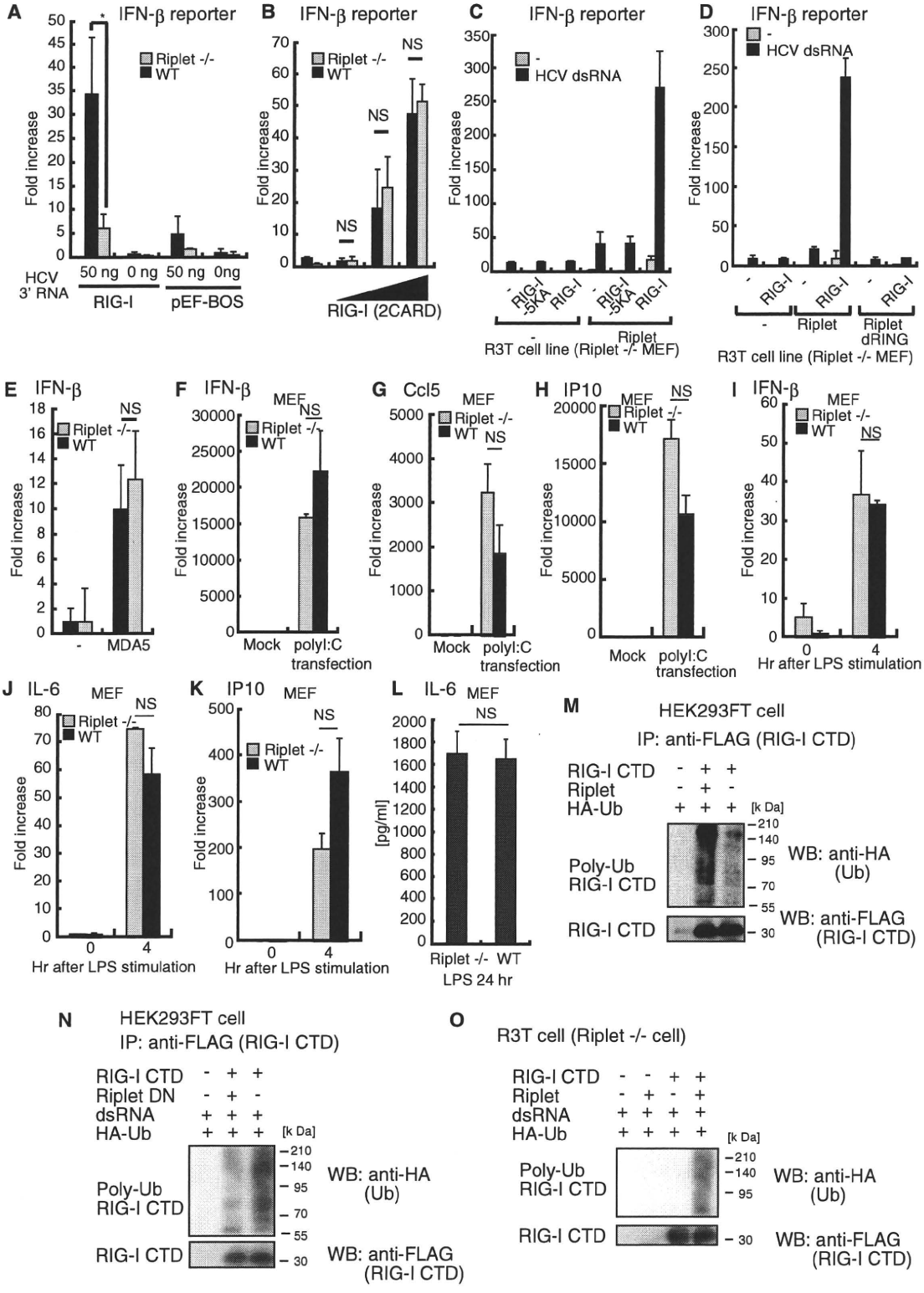

Figure 5. Role of Riplet in the RIG-I-Dependent Pathway

(A) Expression vector of full-length RIG-I and reporter plasmids were transfected into wild-type or *Riplet*$^{-/-}$ MEFs with or without HCV 3′UTR short dsRNA, and after 24 hr IFN-β promoter activation was examined by reporter gene assay. Data are shown as means ±SD and are representative of three independent experiments. *$p < 0.05$ (t test).

is similar to that of RIG-I. Previously, we showed that Riplet binds to RIG-I and mediates Lys63-linked polyubiquitination of RIG-I (Oshiumi et al., 2009). Genetic evidence in this study revealed that Riplet function is essential for RIG-I-dependent type I IFN production. Knockout of Riplet reduced type I IFN production in vivo during the early phase of VSV infection, and *Riplet*$^{-/-}$ mice were susceptible to VSV infection. Taken together, our results provide genetic evidence that Riplet is essential for RIG-I-dependent antiviral immune response in vivo. Most *RIG-I*$^{-/-}$ embryos were lethal at embryonic days 12.5–14.0 in some strain backgrounds (Kato et al., 2005). However, we could not observe any developmental defect in Riplet knockout mice as far as we examined.

Previously, Chen and his colleagues independently isolated Riplet and named it REUL (Gao et al., 2009). They reported that REUL/Riplet binds to RIG-I CARDs but not to CTD (Gao et al., 2009). Furthermore, they reported that REUL/Riplet mediates Lys63-linked polyubiquitination of Lys172 of RIG-I CARDs in a manner similar to TRIM25 (Gack et al., 2007; Gao et al., 2009). Although they did not show any expression profile data for Riplet and TRIM25, they mentioned that TRIM25 and Riplet have different distribution patterns, and thus hypothesized that REUL/Riplet is a complementary factor of TRIM25 and is required for RIG-I activation in cells that do not express TRIM25 (Gao et al., 2009). However, our genetic evidence is not consistent with their hypothesis, because Riplet is essential for RIG-I activation in MEFs that express TRIM25. Previously, Gack et al. showed that knockout of TRIM25 alone abolished RIG-I activation in MEFs (Gack et al., 2007). Therefore, null mutation in either Riplet or TRIM25 abolishes RIG-I activation. This genetic evidence indicates that Riplet can mediate polyubiquitination of RIG-I Lys residues that are not ubiquitinated by TRIM25. This means that Riplet functions differently than TRIM25 in RIG-I activation.

We isolated Riplet cDNA by yeast two-hybrid screening using the C-terminal region of RIG-I (Oshiumi et al., 2009). Because the yeast genome does not encode RIG-I, the interaction indicates the direct binding of Riplet to the RIG-I C-terminal region. The interaction between RIG-I CTD and Riplet has also been confirmed by immunoprecipitation assays in human cells (Oshiumi et al., 2009). Moreover, we have shown that Riplet expression leads to Lys63-linked polyubiquitination of RIG-I CTD (Oshiumi et al., 2009). Recently, Zheng et al. showed that RIG-I CARDs has the ability to bind to polyubiquitin chains (Zeng et al., 2010). We have carefully detected Riplet-mediated polyubiquitination of RIG-I C-terminal region without CARDs, under high-salt conditions, in which many protein-protein interactions were abolished (Oshiumi et al., 2009). Therefore, we proposed the hypothesis that Riplet mediates Lys63-linked polyubiquitination of RIG-I CTD (Oshiumi et al., 2009). This model can explain the genetic evidence that Riplet is essential for RIG-I activation in MEFs that express TRIM25. Gack et al. showed that K172R mutation alone caused near-complete loss of ubiquitination of the human RIG-I CARDs (Gack et al., 2007). Because residue 172 of mouse RIG-I is not Lys but Gln (Shigemoto et al., 2009), Riplet/Reul does not ubiquitinate residue 172 of mouse RIG-I. Based on the previous studies and our current data, we prefer the interpretation that Riplet activates RIG-I through polyubiquitination of RIG-I CTD. However, this interpretation does not exclude the possibility that Riplet ubiquitinates both CTD and CARDs of RIG-I (Gao et al., 2009; Oshiumi et al., 2009).

Previously, we showed that Lys849, -851, -888, -907, and -909 are critical residues in Riplet-mediated RIG-I CTD ubiquitination (Oshiumi et al., 2009). These five Lys residuse are close to the dsRNA binding sites of RIG-I CTD (Takahasi et al., 2008), and the 5KA mutation weakly reduced RNA binding activity of RIG-I. Therefore, it is possible that the 5KA mutation abrogate activation and polyubiquitination of RIG-I by reducing RNA biding activity of RIG-I. However, this possibility is weakened by following observations. First, the 5KA mutation caused near-complete loss of RIG-I activation, but the RIG-I-5KA mutant protein still possessed RNA binding activity. Second, overexpression of Riplet led to RIG-I activation in the absence of dsRNA in HEK293 cells, and this ligand-independent activation of RIG-I

(B) Expression vector for the two RIG-I N-terminal CARDs were transfected into wild-type or *Riplet*$^{-/-}$ MEFs together with reporter plasmids, and IFN-β promoter activation was examined by the reporter gene assay. Data are shown as means ±SD and are representative of three independent experiments. "NS" indicates not statistically significant.

(C) Empty, wild-type RIG-I-, or RIG-I-5KA mutant-expressing vectors were transfected into the *Riplet*$^{-/-}$ MEF cell line together with or without the Riplet-expressing vector. Cells were stimulated with HCV 3′UTR short dsRNA, and reporter gene assay was performed as described in (A).

(D) Empty or wild-type RIG-I-expressing vectors were transfected into the *Riplet*$^{-/-}$ MEF cell line together with empty, wild-type Riplet, or Riplet mutant (Riplet dRING)-expressing vector. Cells were stimulated with HCV 3′UTR short dsRNA, and the reporter gene assay was performed as described in (A).

(E) Empty or MDA5-expressing vectors was transfected into wild-type or *Riplet*$^{-/-}$ MEFs together with reporter plasmids, and after 24 hr IFN-β promoter activation was examined by the reporter gene assay.

(F–H) Of poly(I:C), 0.8 μg was transfected into wild-type or *Riplet*$^{-/-}$ MEFs. Twenty-four hours after transfection, total RNA was extracted from MEFs and subjected to RT-qPCR to determine IFN-β (F), Ccl5 (G), and IP10 (H) expression. Expression in each sample was normalized to the β-actin mRNA expression.

(I–K) Wild-type or *Riplet*$^{-/-}$ MEFs were stimulated with 1 μg of LPS. Total RNA was extracted at the indicated times and subjected to RT-qPCR analysis for of IFN-β (I), IL-6 (J), or IP-10 (K) expression.

(L) Wild-type or *Riplet*$^{-/-}$ MEFs were stimulated with LPS, and after 24 hr the amount of IL-6 in culture supernatants was measured by ELISA.

(M) HEK293FT cells were transfected with Riplet, FLAG-tagged RIG-I-CTD, and HA-tagged ubiquitin (HA-Ub) expression vectors. Twenty-four hours after transfection, cell lysates were extracted and immunoprecipitation was carried out with anti-FLAG antibody as previously described (Oshiumi et al., 2009). The samples were analyzed by SDS-PAGE, and western blotting was performed using anti-HA polyclonal antibody (Ub) and anit-Flag M2 monoclonal antibody (RIG-I-CTD). The plasmids are described previously (Oshiumi et al., 2009).

(N) Expression vector of dominant negative form of Riplet (Riplet DN) was transfected into HEK293FT cells together with expression vector of FLAG-tagged RIG-I CTD and HA-tagged ubiquitin. Cells were stimulated with dsRNA. Ubiquitination of RIG-I CTD was detected as in (M).

(O) R3T cells were transfected with Riplet, FLAG-tagged RIG-I-CTD, and HA-tagged ubiquitin (HA-Ub) expression vectors. Cells were stimulated with dsRNA. Ubiquitination of RIG-I-CTD was detected as in (M).

See also Figure S3.

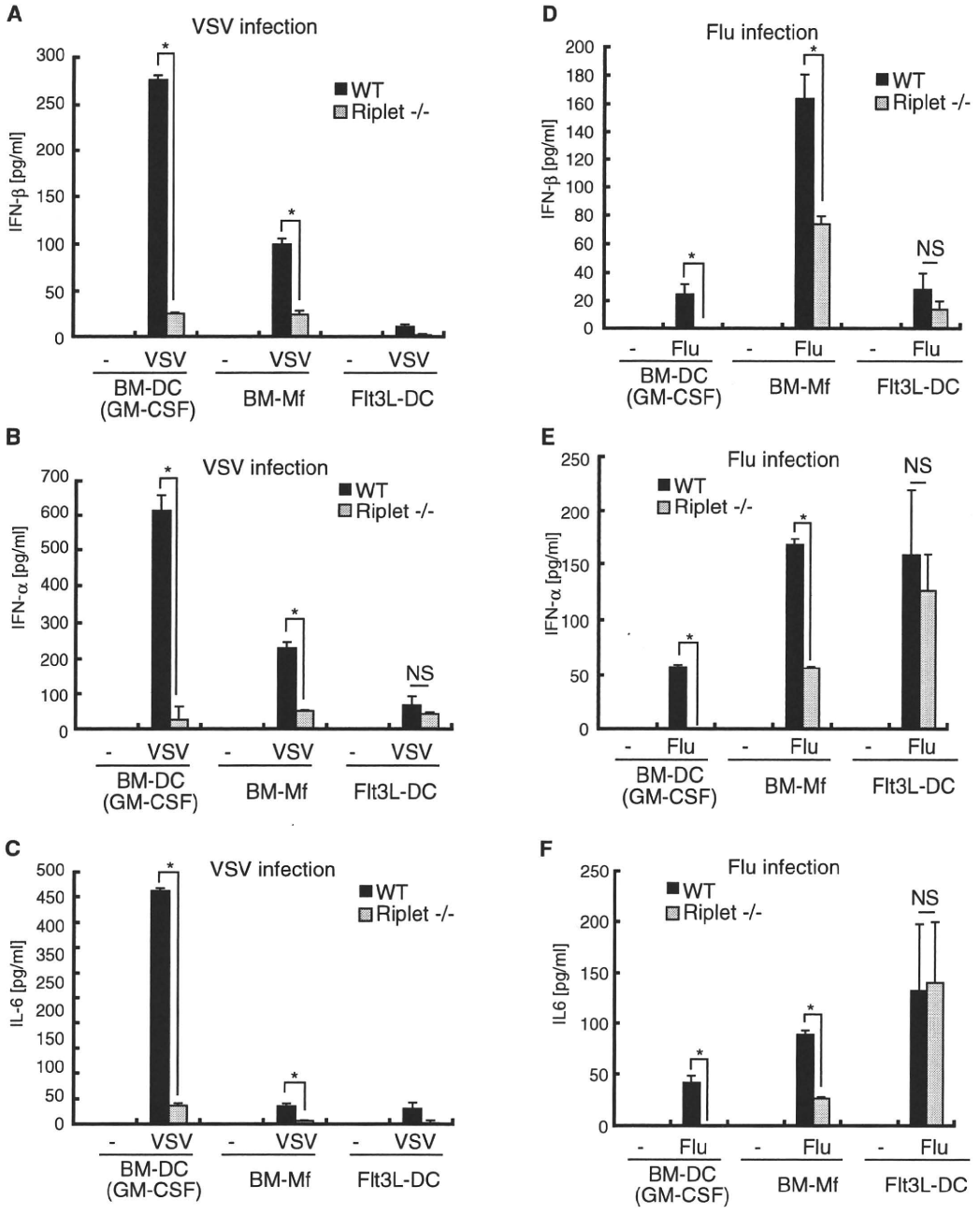

Figure 6. Role of Riplet in Responses to VSV or Flu Infection in Bone Marrow-Derived Cells

GM-DCs, BM-Mf, or Flt3L-DCs were induced from BM-derived cells in the presence of GM-CSF, M-CSF, or Flt3L and infected with VSV or influenza A virus at moi = 1. Twenty-four hours after viral infection, amounts of IFN-β (A and D), -α (B and E), and IL-6 (C and F) in culture supernatants were measured by ELISA. Data are shown as means ±SD and are representative of two independent experiments. *$p < 0.05$ (Student's t test). NS indicates not statistically significant.
See also Figure S4.

by overexpression of Riplet was also abolished by the 5KA mutation. These data support our model. However, we do not exclude the possibility that other Lys residues of RIG-I are ubiquitinated by Riplet, because we have not yet directly detected polyubiquitinated residues of RIG-I CTD by mass spectrometory analysis. Further in vitro studies are required to determine the polyubiquitination sites and to reveal precise RIG-I regulatory mechanisms by Riplet-mediated Lys63-linked polyubiquitation.

In general, E3 ubiquitin ligase targets several types of proteins. Therefore, it is possible that Riplet targets other proteins. Previous work has shown that Riplet binds to the Trk-fused gene (TFG) protein (Suzuki et al., 2001). The TFG protein interacts with TANK and NEMO, which are involved in the NF-κB pathway (Miranda et al., 2006). Although NEMO is involved in IPS-1-mediated signaling, RIG-I CARDs- or MDA5-mediated signaling was normal in *Riplet*$^{-/-}$ MEFs. Therefore, interaction between Riplet

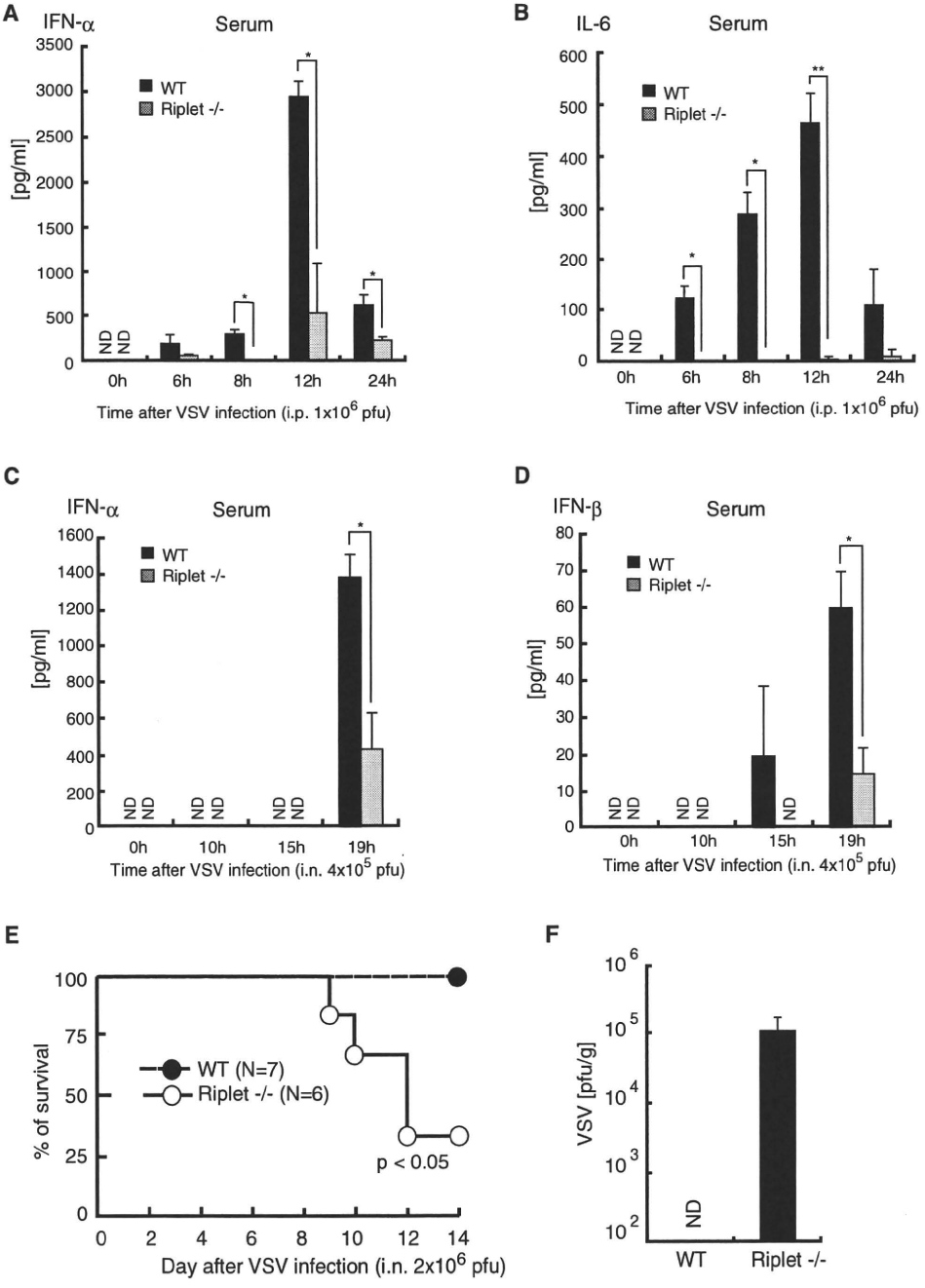

Figure 7. Role of Riplet in Antiviral Responses In Vivo

(A and B) Wild-type or *Riplet*$^{-/-}$ mice were injected intraperitoneally with 1 × 10^6 pfu of VSV. Amounts of IFN-α (A) and IL-6 (B) in mouse serum were measured by ELISA. Data are shown as mean ±SD of samples obtained from three wild-type and three Riplet −/− mice at each time point. *$p < 0.05$ (Student's t test). "ND" indicates not detected.

(C and D) Wild-type and *Riplet*$^{-/-}$ mice were infected intranasally with 4 × 10^5 pfu of VSV. Amounts of IFN-α (C) and IFN-β (D) in mouse serum were measured by ELISA.

(E) Wild-type and *Riplet*$^{-/-}$ mice were infected intranasally with 2 × 10^6 pfu of VSV and mice mortality was observed for 14 days (*$p < 0.05$ between wild-type and *Riplet*$^{-/-}$ mice, log rank test).

(F) Wild-type and *Riplet*$^{-/-}$ mice were infected intranasally with 2 × 10^6 pfu of VSV, and sacrificed for their tissues on day 7 after infection. Titers in brain were determined by the plaque assay. Viral titers in brains of wild-type mice were below 100 pfu/g, and thus not detected (ND). Data are shown as means ±SD (n = 3). See also Figure S5.

and TFG protein is not required for RIG-I-mediated signaling. However, since TFG is involved in tumorigenesis (Miranda et al., 2006), Riplet may be involved in human tumorigenesis.

Several viral proteins inhibit RIG-I-mediated signaling. For example, Flu NS1 inhibits TRIM25 and HCV NS3/4A cleaves IPS-1 (Meylan et al., 2005; Gack et al., 2009). Therefore, Riplet may be inhibited by viral proteins. Indeed, our pilot study indicated that the Riplet protein is disrupted in human hepatocyte cell lines carrying a full-length HCV replicon. RIG-I is involved in innate immune responses against various viruses. In this study, we showed that Riplet is required for innate immune responses against VSV, Flu, and SeV. Therefore, Riplet is also expected to be involved in innate immune responses against other viruses that are recognized by RIG-I.

EXPERIMENTAL PROCEDURES

Generation of Riplet-Deficient Mice

The Riplet gene was amplified by PCR using genomic DNA extracted from ESCs by PCR. The targeting vector was constructed by replacing the second and third exons with a neomycine-resistance gene cassette (Neo), and a herpes simplex virus thymidine kinase (HSV-TK) driven by PGK promoter was inserted into the genomic fragment for negative selection. After the targeting vector was transfected into 129/Sv mice-derived ESCs, G418 and gancyclovir doubly resistant colonies were selected and screened by PCR. The targeted cell line was injected in C57BL/6 blastocysts, resulting in the birth of male chimeric mice. These mice were then crossed with 129/Sv mice to obtain heterozygous mutants. The heterozygous mutants were intercrossed to obtain homozygous *Riplet*$^{-/-}$ mice.

Cells, Viruses, and Reagents

Wild-type and *Riplet*$^{-/-}$ MEFs were prepared from day 12.5–13.5 embryos. *Riplet*$^{-/-}$ MEFs were immortalized with large T antigen and named R3T cell line. BM cells were prepared from 5- to 10-week-old mice. VSV Indiana strain was provided by A. Takada (Hokkaido University). VSV was amplified using Vero cells and the viral titer was determined by the plaque assay. Flu (PR8 strain) and SeV (HVJ strain) was provided by Y. Sakoda (Hokkaido University). HSV-1 strain was provided by K. Kondo (The JIKEI University). Anti-mouse IRF3 antibody was purchased from Zymed. Anti-phospho-STAT1 antibody was purchased from Cell Signaling and anti-STAT1 antibody from Santa Cruz. Salomon sperm dsDNA was purchased from Invitrogen. To determine the viral titer in the brain, the mice were sacrificed, and the brain was aseptically removed and frozen at −80°C. The brain was homogenized in 1 ml of PBS on ice, and the titer was determined by plaque assay.

Preparation of Viral Double-Stranded RNA

cDNA of the HCV 3′UTR region was amplified from total RNA of the HCV genotype 1b full-length replicon using primers HCV-F1 and HCV-R1, and then cloned in the pGEM-T Easy Vector. The primer set sequences were HCV-F1, CTCCAGGTGAGATCAATAGG; and HCV-R1, CGTGACTAGGGCTAAGATGG. RNA was synthesized using T7 and SP6 RNA polymerases. Template DNA was digested by DNase I, and RNA was purified using TRIZOL (Invitrogen) according to manufacturer's instructions.

Quantitative PCR

For qPCR, total RNA was extracted with TRIZOL (Invitrogen) and 0.5 μg of RNA was reverse-transcribed using the High Capacity cDNA Transcription Kit (ABI) with random primers according to the manufacturer's instructions. qPCR was performed using the Step One Real-Time PCR system (ABI). Primer sequences used for qPCR are listed in Table S1.

Measurement of Cytokines

In brief, 5 × 10^5 cells in a 24-well plate were either infected with VSV or Flu, stimulated with LPS, or transfected with HCV 3′UTR dsRNA or poly(I:C). Twenty-four hours after infection, stimulation, or transfection, culture supernatants were collected and analyzed for IFN-α, -β, and IL-6 production by ELISA. Cytokine levels were measured in mouse serum obtained from the mouse tail vein. ELISA kits for mouse IFN-α and -β were purchased from PBL Biomedical Laboratories. ELSA kit for mouse IL-6 was purchased from Invitrogen.

Preparation of Dendritic Cells and Macrophages

BM cells were prepared from the femur and tibia. The cells were cultured in RPMI1640 medium supplemented with 10% FCS, 100 μM 2-Me, and 100 ng/ml human Flt3 ligand (Pepro Tech), and 10 ng/ml murine GM-CSF or culture supernatant NIH 3T3 expressing M-CSF. After 6 days, cells were collected and used as Flt3L-DC, GM-DC, or BM-Mf. In the case of GM-DC or BM-Mf, the medium was changed every 2 days.

Native PAGE Analysis

Approximately 1 × 10^6 MEFs were infected with VSV at moi = 1 for 9 hr and then lysed. Cell lysates in native PAGE sample buffer (62.5 mM Tris-HCl [pH 6.8], 15% glycerol, and BPB) were separated using native PAGE and then immunoblotted with anti-murine IRF3 antibody (Zymed).

Luciferase Assay

Expression plasmids for mouse RIG-I N-terminal CARDs, full-length RIG-I, or full-length MDA5 were constructed in pEF-BOS. The cDNA fragment encoding the ORF of RIG-I or MDA5 was amplified by RT-PCR using total RNA prepared from MEFs. The Riplet dRING mutant protein lacks 1–69 aa region. Wild-type and mutant (Riplet dRING) Riplet-expression vectors were described previously (Oshiumi et al., 2009). Wild-type or *Riplet*$^{-/-}$ MEFs were transiently transfected in 24-well plates with reporter constructs containing the IFN-β promoter and Renilla luciferase (internal control) together with the empty vector (control), RIG-I CARDs, full-length RIG-I, or MDA5 expression vectors. Twenty-four hours after transfection, cells were lysed and subjected to the luciferase assay using the Dual-Luciferase Reporter Assay system (Promega).

Statistical Analyses

Statistical significance of differences between groups was determined by the Student's t test, and survival curves were analyzed by the log rank test using Prism 4 for Macintosh software (GraphPad Sofware, Inc.). Chi-square goodness-of-fit tests and Student's t tests were performed using MS-Excel software and a chi-square distribution table.

SUPPLEMENTAL INFORMATION

Supplemental Information includes five figures, one table, and Supplemental Experimental Procedures and can be found with this article at doi:10.1016/j.chom.2010.11.008.

ACKNOWLEDGMENTS

We thank Dr. John P. Atkinson (Washington University) and Dr. Ralph Steinman (Rockefeller University) for critical discussions, Yoko Esaki and Kiyo Kawata for technical support in generating Riplet KO mice, N. Irie for a pilot study of B-DNA stimulation assay, and Sakoda Y. for technical instructions for the experiments using Flu and SeV. This work was supported in part by the Mitsubishi Foundation; Mochida Foundation; Akiyama Life Science Foundation; and Grants-in-Aid from Ministry of Education, Science, and Culture and Ministry of Health, Labor, and Welfare of Japan.

Received: June 4, 2010
Revised: August 18, 2010
Accepted: November 5, 2010
Published: December 15, 2010

REFERENCES

Akira, S., Uematsu, S., and Takeuchi, O. (2006). Pathogen recognition and innate immunity. Cell *124*, 783–801.

Arimoto, K., Takahashi, H., Hishiki, T., Konishi, H., Fujita, T., and Shimotohno, K. (2007). Negative regulation of the RIG-I signaling by the ubiquitin ligase RNF125. Proc. Natl. Acad. Sci. USA *104*, 7500–7505.

Chiu, Y.H., Macmillan, J.B., and Chen, Z.J. (2009). RNA polymerase III detects cytosolic DNA and induces type I interferons through the RIG-I pathway. Cell *138*, 576–591.

Cui, S., Eisenacher, K., Kirchhofer, A., Brzozka, K., Lammens, A., Lammens, K., Fujita, T., Conzelmann, K.K., Krug, A., and Hopfner, K.P. (2008). The C-terminal regulatory domain is the RNA 5′-triphosphate sensor of RIG-I. Mol. Cell *29*, 169–179.

Diebold, S.S., Kaisho, T., Hemmi, H., Akira, S., and Reis e Sousa, C. (2004). Innate antiviral responses by means of TLR7-mediated recognition of single-stranded RNA. Science *303*, 1529–1531.

Douglas, J., Cilliers, D., Coleman, K., Tatton-Brown, K., Barker, K., Bernhard, B., Burn, J., Huson, S., Josifova, D., Lacombe, D., et al. (2007). Mutations in RNF135, a gene within the NF1 microdeletion region, cause phenotypic abnormalities including overgrowth. Nat. Genet. *39*, 963–965.

Gack, M.U., Shin, Y.C., Joo, C.H., Urano, T., Liang, C., Sun, L., Takeuchi, O., Akira, S., Chen, Z., Inoue, S., and Jung, J.U. (2007). TRIM25 RING-finger E3 ubiquitin ligase is essential for RIG-I-mediated antiviral activity. Nature *446*, 916–920.

Gack, M.U., Kirchhofer, A., Shin, Y.C., Inn, K.S., Liang, C., Cui, S., Myong, S., Ha, T., Hopfner, K.P., and Jung, J.U. (2008). Roles of RIG-I N-terminal tandem CARD and splice variant in TRIM25-mediated antiviral signal transduction. Proc. Natl. Acad. Sci. USA *105*, 16743–16748.

Gack, M.U., Albrecht, R.A., Urano, T., Inn, K.S., Huang, I.C., Carnero, E., Farzan, M., Inoue, S., Jung, J.U., and Garcia-Sastre, A. (2009). Influenza A virus NS1 targets the ubiquitin ligase TRIM25 to evade recognition by the host viral RNA sensor RIG-I. Cell Host Microbe *5*, 439–449.

Gao, D., Yang, Y.K., Wang, R.P., Zhou, X., Diao, F.C., Li, M.D., Zhai, Z.H., Jiang, Z.F., and Chen, D.Y. (2009). REUL is a novel E3 ubiquitin ligase and stimulator of retinoic-acid-inducible gene-I. PLoS ONE *4*, e5760. 10.1371/journal.pone.0005760.

Honda, K., Yanai, H., Takaoka, A., and Taniguchi, T. (2005). Regulation of the type I IFN induction: a current view. Int. Immunol. *17*, 1367–1378.

Honda, K., Takaoka, A., and Taniguchi, T. (2006). Type I interferon [corrected] gene induction by the interferon regulatory factor family of transcription factors. Immunity *25*, 349–360.

Horner, S.M., and Gale, M., Jr. (2009). Intracellular innate immune cascades and interferon defenses that control hepatitis C virus. J. Interferon Cytokine Res. *29*, 489–498.

Hornung, V., Ellegast, J., Kim, S., Brzozka, K., Jung, A., Kato, H., Poeck, H., Akira, S., Conzelmann, K.K., Schlee, M., et al. (2006). 5′-Triphosphate RNA is the ligand for RIG-I. Science *314*, 994–997.

Ishii, K.J., Coban, C., Kato, H., Takahashi, K., Torii, Y., Takeshita, F., Ludwig, H., Sutter, G., Suzuki, K., Hemmi, H., et al. (2006). A Toll-like receptor-independent antiviral response induced by double-stranded B-form DNA. Nat. Immunol. *7*, 40–48.

Ishii, K.J., Kawagoe, T., Koyama, S., Matsui, K., Kumar, H., Kawai, T., Uematsu, S., Takeuchi, O., Takeshita, F., Coban, C., and Akira, S. (2008). TANK-binding kinase-1 delineates innate and adaptive immune responses to DNA vaccines. Nature *451*, 725–729.

Ishikawa, H., and Barber, G.N. (2008). STING is an endoplasmic reticulum adaptor that facilitates innate immune signalling. Nature *455*, 674–678.

Ishikawa, H., Ma, Z., and Barber, G.N. (2009). STING regulates intracellular DNA-mediated, type I interferon-dependent innate immunity. Nature *461*, 788–792.

Kato, H., Sato, S., Yoneyama, M., Yamamoto, M., Uematsu, S., Matsui, K., Tsujimura, T., Takeda, K., Fujita, T., Takeuchi, O., and Akira, S. (2005). Cell type-specific involvement of RIG-I in antiviral response. Immunity *23*, 19–28.

Kato, H., Takeuchi, O., Sato, S., Yoneyama, M., Yamamoto, M., Matsui, K., Uematsu, S., Jung, A., Kawai, T., Ishii, K.J., et al. (2006). Differential roles of MDA5 and RIG-I helicases in the recognition of RNA viruses. Nature *441*, 101–105.

Kawai, T., Takahashi, K., Sato, S., Coban, C., Kumar, H., Kato, H., Ishii, K.J., Takeuchi, O., and Akira, S. (2005). IPS-1, an adaptor triggering RIG-I- and Mda5-mediated type I interferon induction. Nat. Immunol. *6*, 981–988.

Kumagai, Y., Takeuchi, O., Kato, H., Kumar, H., Matsui, K., Morii, E., Aozasa, K., Kawai, T., and Akira, S. (2007). Alveolar macrophages are the primary interferon-alpha producer in pulmonary infection with RNA viruses. Immunity *27*, 240–252.

Kumar, H., Kawai, T., Kato, H., Sato, S., Takahashi, K., Coban, C., Yamamoto, M., Uematsu, S., Ishii, K.J., Takeuchi, O., and Akira, S. (2006). Essential role of IPS-1 in innate immune responses against RNA viruses. J. Exp. Med. *203*, 1795–1803.

Meylan, E., Curran, J., Hofmann, K., Moradpour, D., Binder, M., Bartenschlager, R., and Tschopp, J. (2005). Cardif is an adaptor protein in the RIG-I antiviral pathway and is targeted by hepatitis C virus. Nature *437*, 1167–1172.

Miranda, C., Roccato, E., Raho, G., Pagliardini, S., Pierotti, M.A., and Greco, A. (2006). The TFG protein, involved in oncogenic rearrangements, interacts with TANK and NEMO, two proteins involved in the NF-kappaB pathway. J. Cell. Physiol. *208*, 154–160.

Nakhaei, P., Genin, P., Civas, A., and Hiscott, J. (2009). RIG-I-like receptors: sensing and responding to RNA virus infection. Semin. Immunol. *21*, 215–222.

Onoguchi, K., Yoneyama, M., Takemura, A., Akira, S., Taniguchi, T., Namiki, H., and Fujita, T. (2007). Viral infections activate types I and III interferon genes through a common mechanism. J. Biol. Chem. *282*, 7576–7581.

Oshiumi, H., Matsumoto, M., Hatakeyama, S., and Seya, T. (2009). Riplet/RNF135, a RING finger protein, ubiquitinates RIG-I to promote interferon-beta induction during the early phase of viral infection. J. Biol. Chem. *284*, 807–817.

Pichlmair, A., Schulz, O., Tan, C.P., Naslund, T.I., Liljestrom, P., Weber, F., and Reis e Sousa, C. (2006). RIG-I-mediated antiviral responses to single-stranded RNA bearing 5′-phosphates. Science *314*, 997–1001.

Rehwinkel, J., Tan, C.P., Goubau, D., Schulz, O., Pichlmair, A., Bier, K., Robb, N., Vreede, F., Barclay, W., Fodor, E., and Reis e Sousa, C. (2010). RIG-I detects viral genomic RNA during negative-strand RNA virus infection. Cell *140*, 397–408.

Saito, T., Hirai, R., Loo, Y.M., Owen, D., Johnson, C.L., Sinha, S.C., Akira, S., Fujita, T., and Gale, M., Jr. (2007). Regulation of innate antiviral defenses through a shared repressor domain in RIG-I and LGP2. Proc. Natl. Acad. Sci. USA *104*, 582–587.

Saito, T., Owen, D.M., Jiang, F., Marcotrigiano, J., and Gale, M., Jr. (2008). Innate immunity induced by composition-dependent RIG-I recognition of hepatitis C virus RNA. Nature *454*, 523–527.

Seth, R.B., Sun, L., Ea, C.K., and Chen, Z.J. (2005). Identification and characterization of MAVS, a mitochondrial antiviral signaling protein that activates NF-kappaB and IRF 3. Cell *122*, 669–682.

Shigemoto, T., Kageyama, M., Hirai, R., Zheng, J., Yoneyama, M., and Fujita, T. (2009). Identification of loss of function mutations in human genes encoding RIG-I and MDA5: implications for resistance to type I diabetes. J. Biol. Chem. *284*, 13348–13354.

Sun, Q., Sun, L., Liu, H.H., Chen, X., Seth, R.B., Forman, J., and Chen, Z.J. (2006). The specific and essential role of MAVS in antiviral innate immune responses. Immunity *24*, 633–642.

Suzuki, H., Fukunishi, Y., Kagawa, I., Saito, R., Oda, H., Endo, T., Kondo, S., Bono, H., Okazaki, Y., and Hayashizaki, Y. (2001). Protein-protein interaction panel using mouse full-length cDNAs. Genome Res. *11*, 1758–1765.

Takahasi, K., Yoneyama, M., Nishihori, T., Hirai, R., Kumeta, H., Narita, R., Gale, M., Jr., Inagaki, F., and Fujita, T. (2008). Nonself RNA-sensing mechanism of RIG-I helicase and activation of antiviral immune responses. Mol. Cell *29*, 428–440.

Takeuchi, O., and Akira, S. (2010). Pattern recognition receptors and inflammation. Cell *140*, 805–820.

Xu, L.G., Wang, Y.Y., Han, K.J., Li, L.Y., Zhai, Z., and Shu, H.B. (2005). VISA is an adapter protein required for virus-triggered IFN-beta signaling. Mol. Cell *19*, 727–740.

Yoneyama, M., and Fujita, T. (2009). RNA recognition and signal transduction by RIG-I-like receptors. Immunol. Rev. *227*, 54–65.

Yoneyama, M., and Fujita, T. (2010). Recognition of viral nucleic acids in innate immunity. Rev. Med. Virol. *20*, 4–22.

Yoneyama, M., Kikuchi, M., Natsukawa, T., Shinobu, N., Imaizumi, T., Miyagishi, M., Taira, K., Akira, S., and Fujita, T. (2004). The RNA helicase RIG-I has an essential function in double-stranded RNA-induced innate antiviral responses. Nat. Immunol. *5*, 730–737.

Zeng, W., Sun, L., Jiang, X., Chen, X., Hou, F., Adhikari, A., Xu, M., and Chen, Z.J. (2010). Reconstitution of the RIG-I pathway reveals a signaling role of unanchored polyubiquitin chains in innate immunity. Cell *141*, 315–330.

Frontline

European Journal of Immunology

DEAD/H BOX 3 (DDX3) helicase binds the RIG-I adaptor IPS-1 to up-regulate IFN-β-inducing potential

Hiroyuki Oshiumi, Keisuke Sakai, Misako Matsumoto and Tsukasa Seya

Department of Microbiology and Immunology, Hokkaido University Graduate School of Medicine, Kita-ku, Sapporo, Japan

Retinoic acid-inducible gene-I (RIG-I)-like receptors (RLR) are members of the DEAD box helicases, and recognize viral RNA in the cytoplasm, leading to IFN-β induction through the adaptor IFN-β promoter stimulator-1 (IPS-1) (also known as Cardif, mitochondrial antiviral signaling protein or virus-induced signaling adaptor). Since uninfected cells usually harbor a trace of RIG-I, other RNA-binding proteins may participate in assembling viral RNA into the IPS-1 pathway during the initial response to infection. We searched for proteins coupling with human IPS-1 by yeast two-hybrid and identified another DEAD (Asp-Glu-Ala-Asp) box helicase, DDX3 (DEAD/H BOX 3). DDX3 can bind viral RNA to join it in the IPS-1 complex. Unlike RIG-I, DDX3 was constitutively expressed in cells, and some fraction of DDX3 is colocalized with IPS-1 around mitochondria. The 622-662 a.a DDX3 C-terminal region (DDX3-C) directly bound to the IPS-1 CARD-like domain, and the whole DDX3 protein also associated with RLR. By reporter assay, DDX3 helped IPS-1 up-regulate IFN-β promoter activation and knockdown of DDX3 by siRNA resulted in reduced IFN-β induction. This activity was conserved on the DDX3-C fragment. DDX3 only marginally enhanced IFN-β promoter activation induced by transfected TANK-binding kinase 1 (TBK1) or I-kappa-B kinase-ε (IKKε). Forced expression of DDX3 augmented virus-mediated IFN-β induction and host cell protection against virus infection. Hence, DDX3 is an antiviral IPS-1 enhancer.

Key words: DDX3 · IFN-β · IPS-1 · RIG-I-like receptors · Viral infection

See accompanying Commentary by Mulhern and Bowie

Introduction

Retinoic acid-inducible gene-I (RIG-I) and melanoma differentiation-associated gene 5 (MDA5) are cytoplasmic RNA helicases [1–3], which signal the presence of viral RNA through the adaptor, IFN-β promoter stimulator-1 (IPS-1) (also known as mitochondrial antiviral signaling protein/caspase recruitment domain (CARD) adaptor inducing IFN-β (Cardif)/virus-induced signaling adaptor) to produce IFN-β [4–7]. IPS-1 localizes on the outer membrane of the mitochondria *via* its C-terminus [6]. Its N-terminus consists of a CARD domain, which interacts with the CARD domains of RIG-I and MDA5. Viral RNA resulting from penetration or replication are believed to assemble in the CARD-interacting helicase complex to activate the cytoplasmic IFN-inducing pathway. Although non-infected cells usually express minimal amounts of RIG-I/MDA5, the final output of type I IFN is efficiently induced at an early stage of infection to protect host cells from viral spreading.

Once IPS-1 is activated, the kinase complex consisting of TANK-homologous proteins and virus-activated kinases induce nuclear translocation of IFN regulatory factor-3 (IRF-3) to activate the IFN promoter [8]. NAK-associated protein 1, TANK-binding kinase 1 (TBK1) and I-kappa-B kinase-ε (IKKε) are components of the kinase complex that phosphorylates IRF-3 to induce type I IFN [9, 10]. RIG-I recognizes products of various RNA viruses, while MDA5 recognizes products of picornaviruses

Correspondence: Dr. Tsukasa Seya
e-mail: seya-tu@pop.med.hokudai.ac.jp

[1, 11]. RIG-I and MDA5 share the helicase domain, which is classified into the DEAD (Asp-Glu-Ala-Asp) box helicase family, and the domain can bind to various RNA structures. 5′-triphosphate RNA or short dsRNA is a ligand of RIG-I, whereas long dsRNA is a ligand of MDA5 [1, 12]. However, these RIG-I-like receptors (RLR) are usually up-regulated to a sufficient level secondary to IFN stimulation, suggesting that other molecular mechanisms are responsible for the initial sensing of viral RNA.

Here, we looked for molecules that bind IPS-1 by yeast two-hybrid, and found a DEAD box helicase, DDX3 (DEAD/H BOX 3), as a component of the complex of IPS-1. DDX3 facilitated IPS-1-mediated IFN-β induction to confer high antiviral potential on early infection phase of host cells. This is the first report showing that DDX3 is an IPS-1 complement factor for antiviral IFN-β induction in host infectious cells.

Results

Involvement of DDX3 in the IPS-1 complex

IPS-1 is constitutively present on the mitochondrial membrane and plays a central role in the cytoplasmic IFN-inducing pathway. We searched for proteins that bind IPS-1 in yeast. Using bait plasmids with the IPS-1 CARD region (aa 6–136), we screened a human lung cDNA library to isolate IPS-1 CARD-interacting proteins. We identified one clone, #62 that encodes the DDX3 C-terminal region (aa 276–662), which included partial DEAD box and helicase superfamily C-terminal regions (Fig. 1A). Their interaction was confirmed in HEK293FT cells by immunoprecipitation (IP), where DDX3 and IPS-1 were coupled (Fig. 1B). We confirmed that the C-terminal fragments of DDX3, at least 622-662 a.a, bound IPS-1 (data not shown). Taken together with the results of the yeast two-hybrid assay, the C-terminal portions of DDX3 directly bind the CARD-like region of IPS-1.

RIG-I and MDA5 helicases also bind the IPS-1 CARD domain [4]. In general, RNA helicases make a large molecular complex, and sometimes form homo- or hetero-oligomers. RIG-I binds to LGP2 helicase, and forms homo-oligomers during Sendai virus infection [11]. Hence, we examined whether DDX3 was associated with the RLR proteins by i.p. RIG-I and MDA5 co-precipitated with DDX3 (Fig. 2A), suggesting that DDX3 is involved in the complex of IPS-1 that interacts with RIG-I and/or MDA5. DDX3 bound the C-terminal helicase domain including the RD region of RIG-I (Fig. 2B). Thus, additional interaction may occur between DDX3 and RIG-I/MDA5. IPS-1 localizes to the membrane of mitochondria [6]. Three-color imaging analysis indicated that DDX3 in part co-localized to the IPS-1-mitochodria complex in non-stimulated resting HeLa cells, which express undetectable amounts of RLR (Fig. 2C and data not shown). These results together with accumulating evidence infer that non-infected cells harbor the complex of DDX3 and IPS-1 with minimal amounts of RIG-I/MDA5.

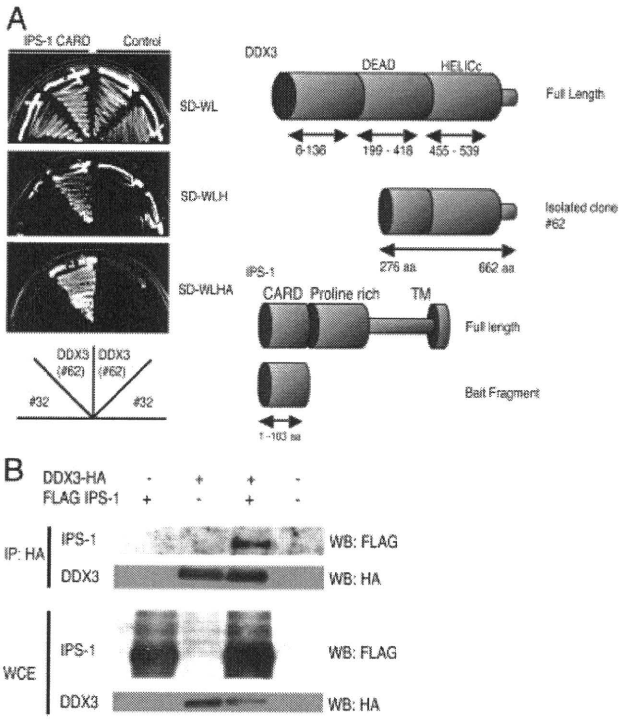

Figure 1. DDX3 binds IPS-1. (A) DDX3 partial cDNA fragment (aa 276–662) isolated by the yeast two-hybrid screening interacted with the IPS-1 CARD region (aa 1–103) in yeast. Tryptophan- and leucine-depleted synthetic dextrose medium plate (SD-WL) is non-selective, and tryptophan-, leucine- and histidine-depleted synthetic dextrose medium plate (SD-WLH) and tryptophan-, leucine-, histidine- and alanine-depleted synthetic dextrose medium (SD-WLHA) plates are selective plates. Empty bait plasmid (pGBKT7) was used for a negative control. (B) FLAG-tagged IPS-1 and HA-tagged DDX3 expression vectors were transiently transfected into HEK293FT cells by FuGeneHD reagent. 24 h after transfection, cell lysates were prepared, and IP was carried out using anti-HA Ab. The immunoprecipitates were analyzed by western blot using anti-HA or FLAG Ab. Data are representative of three independent experiments.

DDX3 promotes IPS-1-mediated IFN-β promoter activation

Forced expression of IPS-1 causes the activation of transcription from the IFN-β promoter. To ascertain the role of DDX3 in IFN-β production, we carried out reporter gene analysis to see the enhancing effect of DDX3 on IPS-1-mediated IFN-β promoter activation. Overexpression of DDX3 alone caused little activation of the promoter; however, the promoter activation was more augmented by minimal addition of DDX3 to IPS-1 than by overexpressed IPS-1 alone (Fig. 3A). This suggested that DDX3 enhanced IPS-1-mediated signaling despite the lack of RIG-I overexpression. To establish which region of DDX3 is important for IFN-β enhancer activity, partial DDX3 fragments were overexpressed with IPS-1, and IFN-β promoter activation was examined. The N-terminal region (aa 1–224, aa 224–487, aa 488–621) barely enhanced promoter activation (data not shown), but the C-terminal region (622–662) activated the promoter (Fig. 3B). These data indicated that the C-terminal region of DDX3 is important for the binding to IPS-1 and potentiation of the IPS-1 pathway.

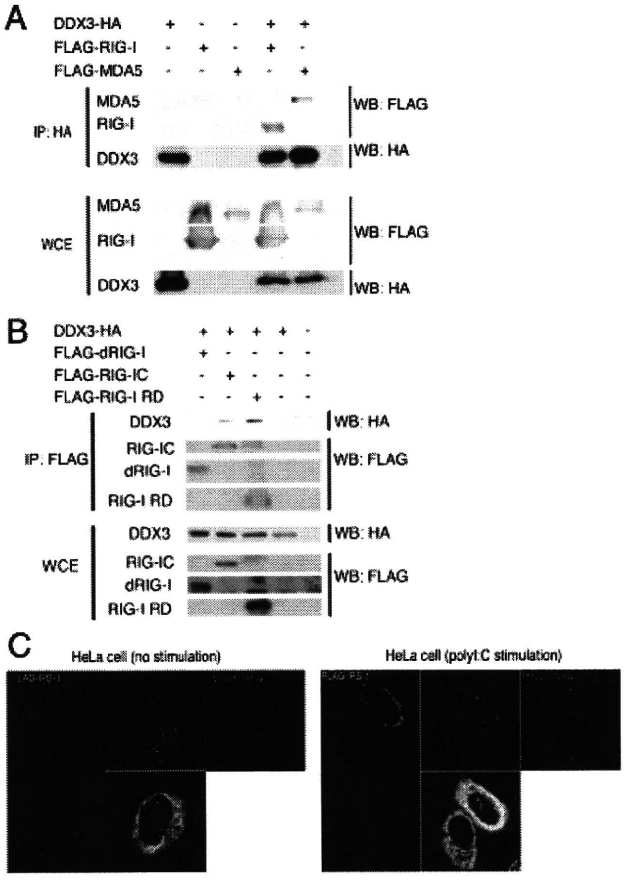

Figure 2. DDX3 joins the complex of RIG-I, MDA5 and IPS-1. (A) RIG-I and MDA5 co-precipitate with DDX3. HA-tagged DDX3 was expressed in HEK293FT cells, together with FLAG-tagged MDA5 or RIG-I, and 24 h after transfection, IP was performed using anti-HA Ab and analyzed by western blotting. (B) The C-terminal region of RIG-I participates in complex formation with DDX3. FLAG-tagged RIG-I fragments and HA-tagged DDX3 were expressed in HEK293 cells, and 24 h after transfection, IP was performed using anti-HA Ab and analyzed by western blotting. (C) DDX3 colocalizes with IPS-1. Flag-tagged IPS-1 and HA-tagged DDX3 were transfected into HeLa cells together with or without polyI:C. After 24 h, cells were fixed with formaldehyde and stained with anti-HA polyclonal and anti-FLAG monoclonal Ab. Alexa488 (DDX3-HA) or Alexa633 Ab was used for second Ab. Mitochondria was stained with Mitotracker Red. DDX-3 partially colocalized with IPS-1. Data are representative of three independent experiments.

DDX3 as a component of initial RNA sensor

RIG-I and MDA5 are IFN-inducible proteins, only traces of which exist in an early phase (<2 h) in the cytoplasm where viral RNA replicate. Previous reports showed that DDX3 binds RNA of poly rA or duplexed RNA [13, 14], and our protein analysis solidified this issue: DDX3 efficiently bound polyI:C and stem-loop RNA of viral origin in a solution (data not shown). DDX3 as well as IPS-1 were expressed even without any stimulation (Fig. 2C and 4A and B) and bound each other in the cytoplasm (Fig. 2C). Hence, DDX3 is a cytoplasmic molecule that can detect viral RNA produced in infected cells.

Knockdown studies suggested that polyI:C-mediated IFN promoter activation was abrogated in DDX3-deficient cells even in the presence of overexpressed RIG-I or MDA5 (Fig. 5). DDX3 silencing happened with two different siRNA. Thus, DDX3 may enable RIG-I and IPS-1 to confer activation of the cytoplasmic RNA-sensing pathway on virus-infected cells.

The IFN-β-inducing pathway involves IRF-3 kinases TBK1 and IKKε, which may be targets of DDX3 [15, 16]. By *in vitro* reporter analysis, increasing amounts of DDX3 barely affected IFN-β promoter activation by TBK1 and IKKε (Fig. 6A and B). Slight TBK1-enhancing activity could manage to be detected with DDX3 when decreasing amounts of TBK1 was used in the assay (Fig. 6C and D).

HeLa cells induced the mRNA of RIG-I and IFN-β in response to polyI:C stimulation within 1 h (Fig. 4A). More exactly, IFN-β induction was ~30 min faster than RIG-I induction in response to polyI:C. IFN-β mRNA induction was peaked around 3 h post stimulation, while RIG-I induction continued to increase >3 h (Fig. 4A). When HEK293 cells were infected with vesicular stomatitis virus (VSV) (a RIG-I-stimulating virus), the IFN-β mRNA was induced from 6 h, and by that time no RIG-I message was generated (Fig. 4B–D). The RIG-I message began to appear >8 h and was markedly increased (Fig. 4B and D). In either case, no up-regulation was observed with DDX3 but sufficiently present in the cytoplasm (Fig. 4C). Furthermore, overexpression of DDX3 in HeLa cells resulted in potential prevention of VSV propagation (Fig. 7). However, the distribution profiles of DDX3 and IPS-1 were barely altered in response to polyI:C stimulation (Fig. 2C). The results allow us to interpret that when viral RNA enter the cytoplasm of infected cells, the RNA first induce a small amount of IFN-β in conjunction with the complex containing trace RIG-I and then the induced IFN-β fosters intensive RIG-I/MDA5 induction. The complex is reconstituted together with upcoming RIG-I/MDA5 to amplify the cytoplasmic IFN-inducing pathway. Although the molecular reconstitution was not visible with overexpressed proteins by confocal analysis, DDX3 may act as an enhancing factor for initial RNA-sensing by the IPS-1 complex and conducts the rapid response to viral RNA to facilitate the IPS-1 signaling.

Discussion

We identified DDX3 as a protein that bound to the IPS-1 CARD region, duplexed RNA and RLR. Although the DDX3 helicase domain is a DEAD box type similar to those of RIG-I and MDA5, DDX3 does not have a signaling domain corresponding to the CARD domain. Therefore, DDX3 may not act as a signal sensor of RNA viruses, as RIG-I and MDA5 do. Considering the role of DDX3 in host RNA metabolism, it is more likely that DDX3 acts as a scaffold for RIG-I (even under the presence of low copy numbers of RIG-I) and intensifies IPS-1 signaling similar to LGP2 [11, 17]. RNA molecules usually form a complex with various

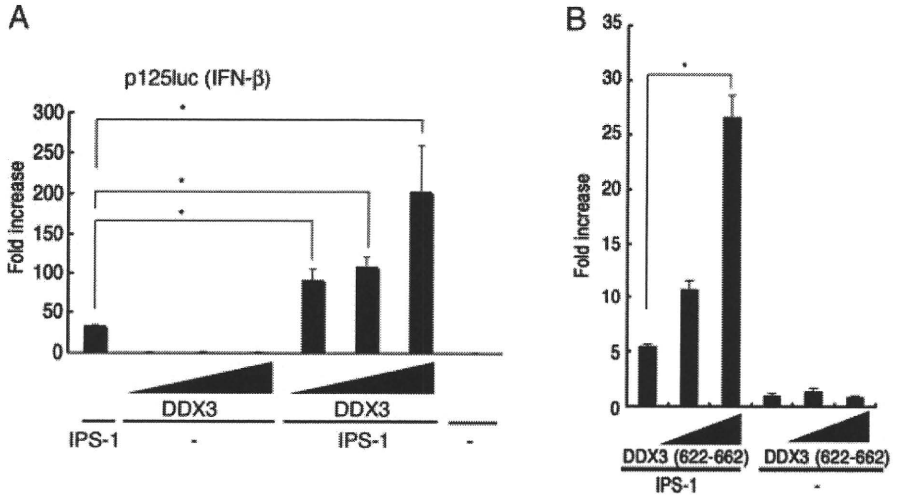

Figure 3. The C-terminal region of DDX3 participates in enhancing IPS-1-mediated IFN-β promoter activation. (A) Activation of IFN-β promoter was examined by reporter gene assay. HEK293 cells were transfected with DDX3- (100, 200 or 300 ng) and/or IPS-1 (100 ng)-encoding plasmids, together with reporter (p125luc) and control plasmids (Renilla luciferase) into 24-well plates. (B) The plasmids for expression of DDX3 (622-662 aa) and IPS-1 or the former only were transfected into HEK293 cells in 24-well plates together with p125luc reporter plasmid. After 24 h, the activation of reporter was measured. Data show mean fold induction+SD of three independent assays. $^*p<0.05$, Student's *t*-test.

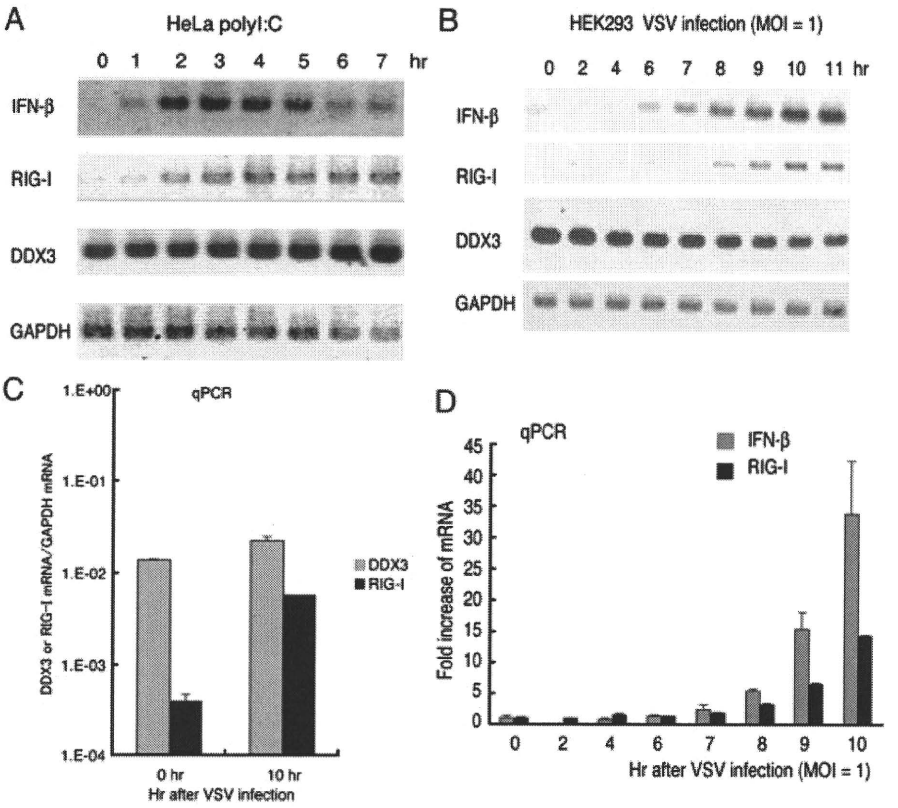

Figure 4. Earlier induction of IFN- than RIG-I in virus-infected cells. (A) Early induction of IFN-β in response to polyI:C. HeLa cells were stimulated with 50 μg/mL of polyI:C for indicated hours. Total RNA was extracted with TRIZOL and RT-PCR was carried out to examine the kinetics of expressions of DDX3, IFN-β, RIG-I and GAPDH (control). (B) IFN-β mRNA induction by VSV infection. HEK293 cell were infected with VSV at MOI = 1, and then total RNA was extracted with TRIZOL reagents at indicated times. The reverse transcription with random primers and PCR at 33 cycle were performed to detect RIG-I, DDX3 or IFN-β expression. Data are representative of three independent experiments. (C) Marked induction of RIG-I in VSV-infected cells. HEK293 cells were infected with VSV at MOI = 1, and then the total RNA was extracted with TRIZOL reagent at indicated times. The relative amounts of RIG-I or DDX3 mRNA were quantified by RT-qPCR, in which the mRNA of GAPDH was used for endogenous internal control. (D) Fold increase of IFN-β or RIG-I mRNA by VSV infection. The amount of IFN-β or RIG-I cDNA was determined by quantitative PCR. The fold increases were calculated by dividing the values of each time point by that of 0 h sample of IFN-β or RIG-I. Data show mean+SD pooled from three independent experiments.

proteins, such as 5′-end capping enzymes or translation initiation factors. Viral RNA also tends to couple with host proteins to replicate and translate RNA. DDX3 capturing RNA may function either in the molecular complex of RIG-I/MDA5/IPS-1 or in the complex of the translation machinery.

Recently, DDX3 was reported to up-regulate IFN-β induction by interacting with IKKε in the kinase complex [18]. IKKε is an NF-κB-inducible gene, whereas the DDX3-IPS-1 complex is constitutively present prior to infection. DDX3 may bind IKKε after IKKε is generated secondary to NF-κB activation [15]. Another report suggested that DDX3 interacts with TBK1 to synergistically stimulate the IFN-β promoter [16]. The report further suggested that DDX3 is recruited to the IFN promoter and acts like a transcription factor [16]. These reports also show that not C-terminal but N-terminal region of DDX3 is required for enhancing the IKKε- or TBK1-mediated IFN promoter activation. We showed that unlike these previous reports, the C-terminal region of DDX3 is important for the IPS-1 activation. These observations indicate that DDX3 is involved in RIG-I signaling at multiple steps. The involvement of DDX3 at several steps is not surprising, because DDX3 plays several roles in RNA metabolisms, such as RNA translocation or mRNA translation.

In cytoplasm, there are large amounts of DDX3 and only trace amounts of RIG-I in resting cells. Therefore, when the virus initially infects human cells, the viral RNA would encounter DDX3 before RIG-I capture the viral RNA. We demonstrated that the initial IPS-1 complex for RNA-sensing involves DDX3 in addition to trace RIG-I to cope with the early phase of infection. This IPS-1 complex activates downstream signal by involving a minute amount of viral RNA. What happens in actual viral infection is to first induce IFN-β and then RIG-I (Fig. 4B), suggesting that the initial IFN-β mRNA arises independent of the virus-induced RIG-I. Once IFN-β and RIG-I mRNA are up-regulated by viral RNA, the IPS-1 complex turns constitutionally different: the complex contains high amounts of RIG-I, which may directly capture viral RNA without DDX3. Our results indicate that the early IPS-1 complex formed in the early stages of virus-infected cells induce minute IFN-β with a mode different from the conventional IPS-1 pathway that RIG-I solely capture viral RNA and activates IPS-1. By retracting DDX3 from the complex by siRNA, only a minimal IFN-β response emerges merely with preexisting RIG-I and IPS-1, suggesting DDX3 to be a critical signal enhancer in the early IPS-1 complex. Development of a method to chase endogenous DDX3 will be required to test our interpretation.

The RIG-I generation occurring >8 h post RNA virus challenge makes the complex direct the conventional IFN-inducing pathway harboring sufficient RIG-I/MDA5. Previous reports [13, 14] and our RNA-binding analysis also speculated that one of the RNA-capture proteins is DDX3 since DDX3 tightly binds polyI:C and dsRNA in fluid phase. These RNA-capture proteins may have a role in the IPS-1-involving molecular platform in cells with early virus infection when only a trace RIG-I protein is expressed. This interpretation fits the result that DDX3 acts predominantly on an early phase of virus infection (Fig. 4B and 7).

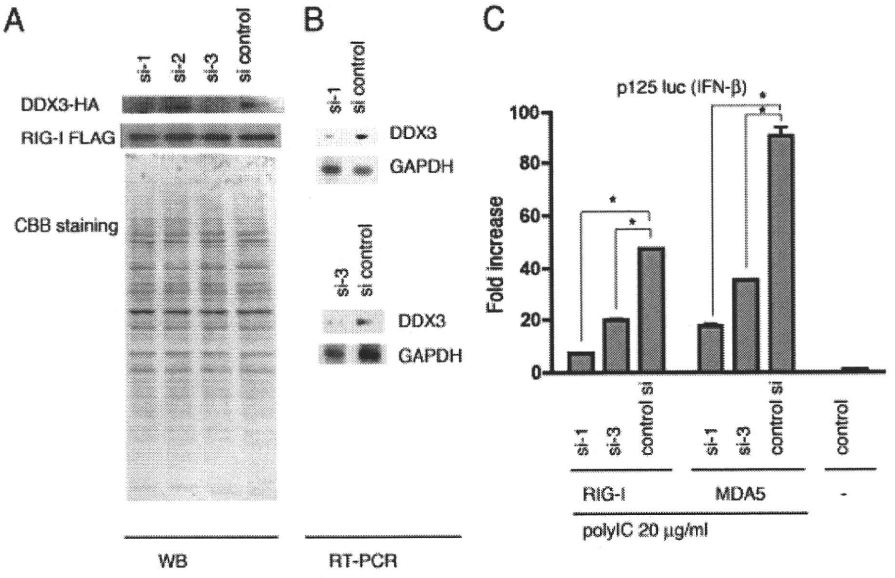

Figure 5. Knockdown of DDX3. (A) Negative control or DDX3 targeting siRNA (20 pmol), DDX3 si-1, -2 or -3, were transfected into HEK293 cells in 24-well plates, together with HA-tagged DDX3 or FLAG-tagged RIG-I expression plasmids, and after 48 h, cell lysates were prepared and analyzed by western blotting with anti-HA or anti-FLAG Ab, and the same membrane was stained with CBB. (B) DDX3 si-1, -3 or control siRNA was transfected into HEK293 cells, and after 48 h, expression of endogenous DDX3 mRNA was examined by RT-PCR. (C) DDX3 si-1, -3 or control siRNA was transfected into HEK293 cells with reporter plasmids and RIG-I- or MDA5 expression plasmid (100 ng). Forty-eight hours after transfection, cells were stimulated with polyI:C (20 μg/mL) with dextran for 4 h, and activation of the reporter was measured. siRNA for DDX3 reduced RIG-I- or MDA5-mediated p125luc activation. Data are representative of three independent experiments (A,B). Data show mean fold increase+SD pooled from three independent experiments (C). *$p<0.05$, Student's t-test.

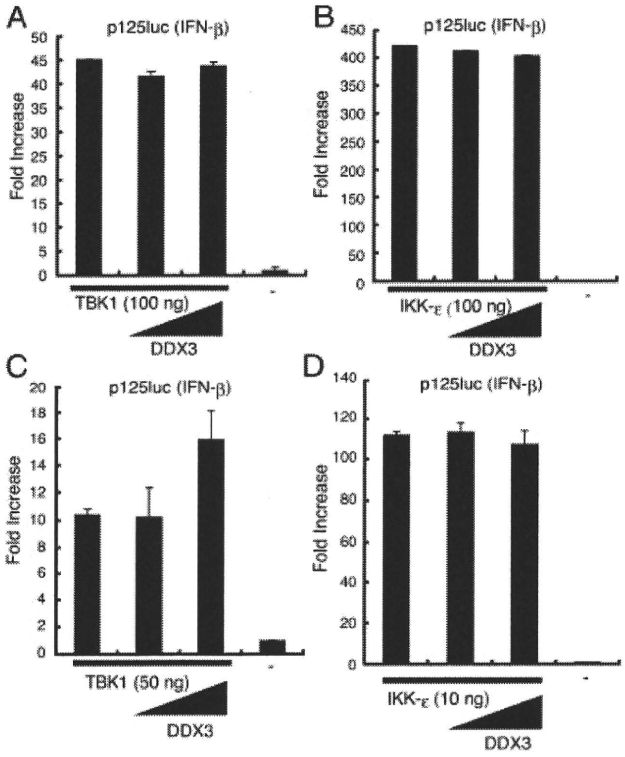

Figure 6. TBK1 and IKKε are not main targets for DDX3-mediated IFN-β up-regulation. (A–D) The activation of IFN-β promoter was examined by reporter gene assay. HEK293 cells were transfected in 24-well plates with DDX3 (0, 100 or 300 ng)-, TBK1 (0, 50 or 100 ng)- or IKKε (0, 10 or 100 ng)-encoding plasmid together with reporter (p125luc) and control plasmid. After 24 h, the cell lysate was prepared and the luciferase activities were measured. Data show mean+SD of three independent experiments.

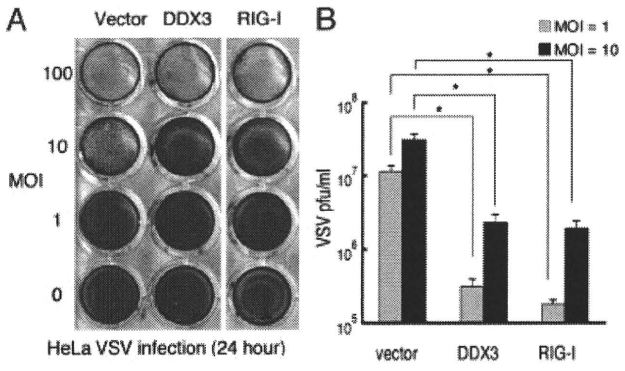

Figure 7. VSV infection is suppressed by overexpressed DDX3. (A) HeLa cells were transfected with DDX3, RIG-I or empty vector. After 24 h, the transfected cells were infected with VSV at indicated MOI. 24 h after VSV infection, the cells were fixed with formaldehyde and stained with crystal violet. (B) The VSV titers of culture supernatant of HeLa cells infected with VSV at MOI = 1 or 10 were measured by plaque assay. Data show mean+SD of three independent experiments. *$p<0.05$, Student's *t*-test.

Proteins involved in type I IFN induction are found ubiquitinated for their functional regulation. It has been reported that TRIM25 [19] and Riplet/RNF135 [20] act as ubiquitin ligases to activate RIG-I for IFN-β induction in their different sites of RIG-I ubiquitination. Another ubiquitin ligase RNF125 polyubiquitinates RIG-I through Lys48, leading to degradation of RIG-I [21]. The RIG-I level is highly susceptible to not only IFN but also ubiquitination in host cells. In addition, many viral factors may suppress the RIG-I function. It remains unknown what factor maintains a minimal level of RIG-I/MDA5 in resting cells. We favor the interpretation that DDX3 can be an alternative factor for compensating the low RLR contents in a certain infectious situation such that RIG-I is degraded or poorly up-regulated by other viral factors.

DDX3 is functionally complicated since its protective role against viruses may be modulated after the synthesis of viral proteins. DDX3 couples with the HCV core protein in HCV-infected cells and promotes viral replication [22]. This alternative function of DDX3 is accelerated by the HCV core protein, since the core protein withdraws DDX3 from the IFN-β-inducing facility, leading to suppression of IFN-β induction and positive regulation of HCV propagation in infected cells. DDX3 is also involved in HIV RNA translocation [14]. The DDX3 gene is conserved among eukaryotes, and Ded1 is a budding yeast homolog [23]. Ded1 helicase is essential for initiation of host mRNA translation, and human DDX3 can complement the lethality of Ded1-null yeast cells [24, 25]. Hence, another function of DDX3 is to bind viral RNA to modulate RNA replication and translocation. It is not surprising that DDX3 is implicated in various steps of RNA metabolism in cells with both host and viral RNA.

Materials and methods

Cell culture and reagents

HEK293 cells and HEK293FT cells were maintained in Dulbecco's Modified Eagle's low or high glucose medium (Invitrogen, Carlsbad, CA, USA) supplemented with 10% heat-inactivated FBS (Invitrogen) and antibiotics. HeLa cells were maintained in MEM (Nissui, Tokyo, Japan) supplemented with 10% heat-inactivated FBS. Anti-FLAG M2 mAb, anti-HA polyclonal Ab, were purchased from Sigma-Aldrich (St. Louis, MO, USA). Alexa Fluor®-conjugated secondary Ab were from Invitrogen.

Plasmids

DDX3 cDNA encoding the entire ORF was cloned into pCR-blunt vector using primers, DDX3N F-Xh (CTC GAG CCA CCA TGA GTC ATG TGG CAG TGG AA) and DDX3C R-Ba (GGA TCC GTT ACC CCA CCA GTC AAC CCC) from human lung cDNA library. To make an expression plasmid, HA tag was fused at the C-terminal end of the full length DDX3 (pEF-BOS DDX3-HA). pEF-BOS DDX3 (1–224 aa) vector was made by using primers DDX3 N-F-Xh and DDX3D1 (GGA TCC GGC ACA AGC CAT CAA GTC TCT TTT C).